Highly Absorptive Thin Films for

Integrated Photonic Devices

by

Michael Scott Bradley

S. B. Electrical Science and Engineering (2004)

Massachusetts Institute of Technology

Submitted to the Department of Electrical Engineering and Computer Science

in Partial Fulfillment of the Requirements for the Degree of

Master of Engineering in Electrical Engineering and Computer Science

at the Massachusetts Institute of Technology

February 3, 2006

Author_____
Department of Electrical Engineering and Computer Science
February 3, 2006

Certified by_____
Vladimir Bulović
Thesis Supervisor

Accepted by_____
Arthur C. Smith
Chairman, Department Committee on Graduate Theses

Table of Contents

Table of Figures

Highly Absorptive Thin Films for

Integrated Photonic Devices

by
Michael Scott Bradley

Submitted to the
Department of Electrical Engineering and Computer Science

February 3, 2006

In Partial Fulfillment of the Requirements for the Degree of
Master of Engineering in Electrical Engineering and Computer Science

ABSTRACT

Highly absorptive thin films serve as the active layer of a new class of photonic devices based on the strong coupling of light and matter. In order to develop these devices into a new field of integrated photonics, methods for analysis, patterning, and deposition of the active layer are necessary. This thesis develops these methods and applies them to thin films of J-aggregates grown in a layer-by-layer (LBL) process, which have been shown to have remarkable optical and morphological properties and have recently enabled the demonstration of strong coupling between light and matter in an electroluminescent device at room temperature. J-aggregate thin films are analyzed using Kramers-Kronig regression to determine their complex index of refraction, an important parameter involved in photonic device design. Additionally, a soft lithography method is demonstrated for patterning and deposition of LBL J-aggregate thin films. Together, these methods can be used to further enable integrated photonics based on the strong coupling of light and matter.

Thesis Supervisor: Vladimir Bulović
Title: Associate Professor of Electrical Engineering

I. Introduction

A material that forms highly absorptive thin films has distinct potential for use in photonic devices. With a small input signal, electrical or optical, a large change in the film's optical properties can be realized. Generally, to realize this large change in inorganic semiconductors, the devices must be cooled significantly due to a high density of mobile electrons in the material. Without this cooling, the effects of the input signal are quickly lost due to electronic rearrangement, known as dephasing. Organic semiconductors, unlike their inorganic counterparts, generally have a very low density of mobile electrons, meaning that the effects of an input signal are more persistent. However, as is usually the case in engineering, a trade-off generally occurs when moving from an inorganic to organic system: organic semiconductors generally have low oscillator strength. This thesis describes research involving an organic material that mitigates the above trade-off and combines the high oscillator strength typically found in inorganic semiconductors with the low dephasing effects found in organic semiconductors. This material, J-aggregates of cyanine dyes, can be formed into nanometer-scale thin films with very high absorption constants. Recent work with J-aggregate thin films has shown that it is possible to realize the strong quantum coupling of the states of the electric field in an optical microcavity with the electronic states in J-aggregate thin films, potentially allowing for an entirely new class of photonic devices.[1-7] This thesis explores methods of analyzing, patterning, and depositing highly absorptive thin films, applied to those of J-aggregates, that could help further the realization of this new class of photonic devices based on the strong coupling of light and matter.

There are two main sections in this thesis following the introduction. The introduction provides background information regarding J-aggregates and the layer-by-layer (LBL) method used throughout this thesis for forming J-aggregate thin films. Following the introduction, the first section discusses the analysis of highly absorptive thin films, applied to those of J-aggregates, in order to determine the films' complex index of refraction, which is a necessary parameter in the design of photonic devices. The second section discusses research in the patterning and deposition of J-aggregate thin films in a microcontact printing (μCP) process. Especially in the case of highly absorptive organic thin films, like those of J-aggregates, μCP is a useful patterning and deposition method. In patterning, μCP eliminates a reactive etch step which can significantly damage organic thin films. In deposition, μCP decouples the formation and deposition of an organic thin film. Because the film is formed on the stamp, the device substrate does not have to be exposed to the possibly harsh growth environment of the film. Together, the methods of analysis, deposition, and patterning described in these sections form a framework for creating integrated photonic devices and show the application of the methods to thin films of J-aggregates.

I.A. J-Aggregates

J-aggregates, short for Jelley aggregates, have found extensive use in industry because of their optical and electronic properties. In the photographic film industry of the 20th century, J-aggregates were widely use as sensitizers for silver halides.[8] J-aggregates were first reported by Edwin Jelley of Kodak in a letter to the journal *Nature* in 1936.[9] The materials were further researched by G. Scheibe, and because of his work J-aggregates are also at times referred to as Scheibe aggregates.[10] The term "J-

aggregate" generally refers to any aggregation of molecules in which the transition dipoles of the molecules align in such a way that the transition dipole of the entire aggregate is larger than that of a single molecule. This alignment effectively delocalizes an exciton across the molecules of an aggregate. The enhancement of the overall dipole in a J-aggregate is special among organic materials since the formation of aggregates is generally linked to a lower overall transition dipole since the individual dipoles usually cancel each other.[11]

The first use of J-aggregates for the purpose of strongly coupling light and matter was reported by Lidzey *et al.* in a letter to *Nature* in 1998.[1] Lidzey *et al.* demonstrated that the formation of a polaritonic band gap could be realized at room temperature using a J-aggregate thin film placed in an optical microcavity. A polariton is the term applied to the quantum mechanical quasi-particle formed by coupling an exciton, itself a quasi-particle, to a photon. Whereas for a usual microcavity there is only one resonant reflectance dip or transmittance peak, formation of a polaritonic band gap is indicated by the appearance of two peaks centered about the original cavity resonance, which disappears. The range between the two new peaks is referred to as the polaritonic band gap.[5] Since Lidzey *et al.*'s demonstration, further research has been done in exploring Lidzey *et al.*'s device structure, and additional device structures have been proposed and demonstrated. For example, the first room-temperature electroluminescence from a strongly-coupled J-aggregate thin film in an organic light-emitting device (OLED) structure was demonstrated in 2004 by Tischler *et al.*[6,7] Together, the above research has shown J-aggregates to be a promising highly-absorptive material for use in an entirely new class of photonic devices based on the strong coupling of light and matter.

J-aggregate thin films are commonly formed using one of three techniques: Langmuir-Blodgett, spin-casting in a polymer matrix, and LBL deposition.[12-14] The last technique is the newest, having first been reported by Fukumoto and Yonezawa in 1998. For his electroluminescent devices, Tischler used thin films of J-aggregates formed with the LBL deposition method, and his work suggested that highly absorptive thin films of J-aggregates could be engineered using the LBL technique. The work with J-aggregate thin films by Tischler was a starting point for the research reported in this thesis, and LBL J-aggregate thin films like those used by Tischler are the primary focus of the analysis, patterning, and deposition methods developed in this text.

I.B. Layer-by-Layer Deposition

The LBL deposition method has been an active field of materials science research in the past decade since it was first reported by Decher *et al.*[14-23] A basic LBL process consists of dipping a substrate in alternating polycation and polyanion solutions. Substrates undergo these sequential immersions in cationic and anionic solutions (SICAS) in order to build up a thin film, one layer of polymer at a time. The polycations and polyanions can be either strong or weak. This classification refers to the pH-sensitivity of the polyelectrolytes. Strong polyelectrolytes are not pH sensitive, whereas the charge on weak polyelectrolytes depends on the pH of the solvent. Between dips in the polycation and polyanion solutions, the substrates are rinsed, typically in the same solvent used for the polycation and polyanion, in order to remove excess polymer that has not been ionically bonded to the substrate. The substrate must be prepared in some manner that allows the first adsorption step to occur. For glass substrates, an oxygen plasma treatment generally leaves enough negative charge on the surface (assuming the

polycation solvent is a weak acid or base) such that enough polycation can adsorb for the build-up process to start.

While the LBL process was developed with polycations and polyanions as the thin film constituents, further work in the 1990s showed that one of the polyelectrolytes could be replaced by a dye molecule or other small, charged component.[20] The only requirement of the charged component was that enough of the component adsorb in the LBL process to reverse the charge on the surface of the substrate. This requirement is easily satisfied if the charged component is multivalent or if the charged component will form aggregates. Fukumoto and Yonezawa showed that, by using J-aggregating cyanine dyes as one of the charged components, thin films of J-aggregates could be built using the LBL process. Figure I.1 shows a schematic of a typical LBL process used in this study. The polycation is PDAC (poly(diallyldimethylammonium chloride)), which is a strong polyelectrolyte, and the anion is the J-aggregating cyanine dye TDBC (5,6-dichloro-2-[3-[5,6-dichloro-1-ethyl-3-(3-sulfopropyl)-2(3H)-benzimidazolidene]-1-propenyl]-1-ethyl-3-(3-sulfopropyl) benzimidazolium hydroxide, inner salt, sodium salt from Nippon Kankoh Shikiso Kenkyusho Co., Ltd.). TDBC is used throughout this project. A diagram of a TDBC molecule is shown in Figure I.2, showing the linear structure typical of J-aggregating cyanine dye molecules.

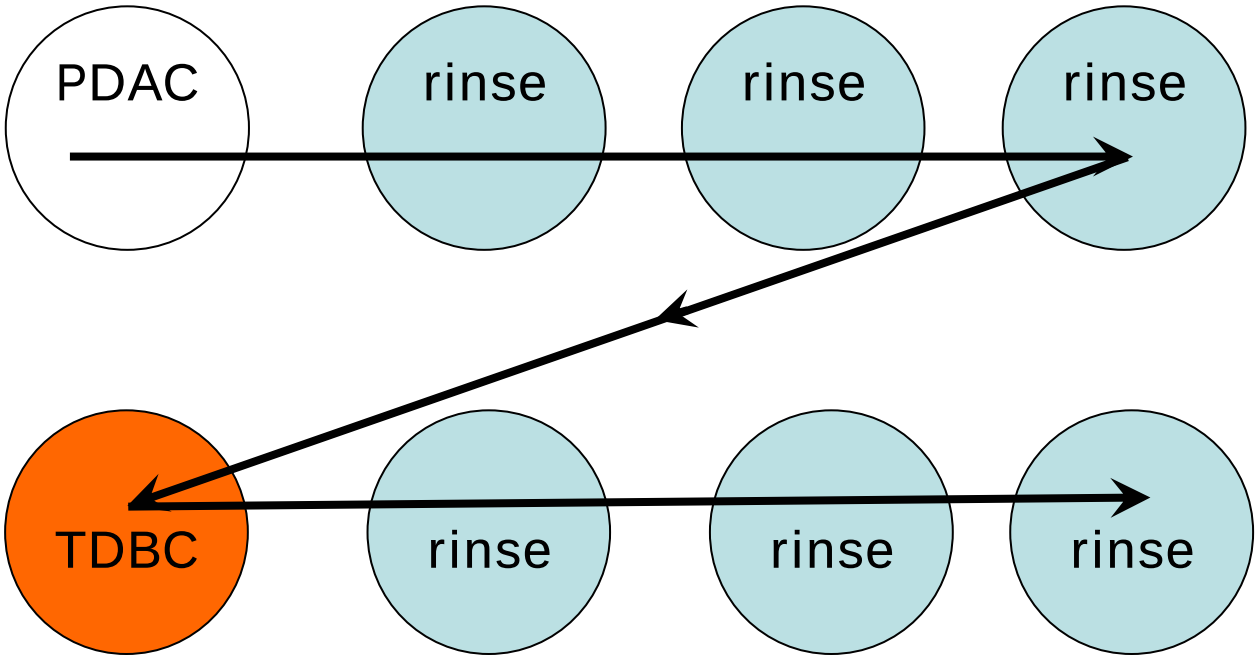

Figure I.1 Schematic of a typical LBL cycle, one sequential immersion in cationic and anionic solutions (SICAS), used in this project. The substrate is dipped into the polycation PDAC, followed by three rinses, and then dipped into the anion TDBC, followed by three rinses.

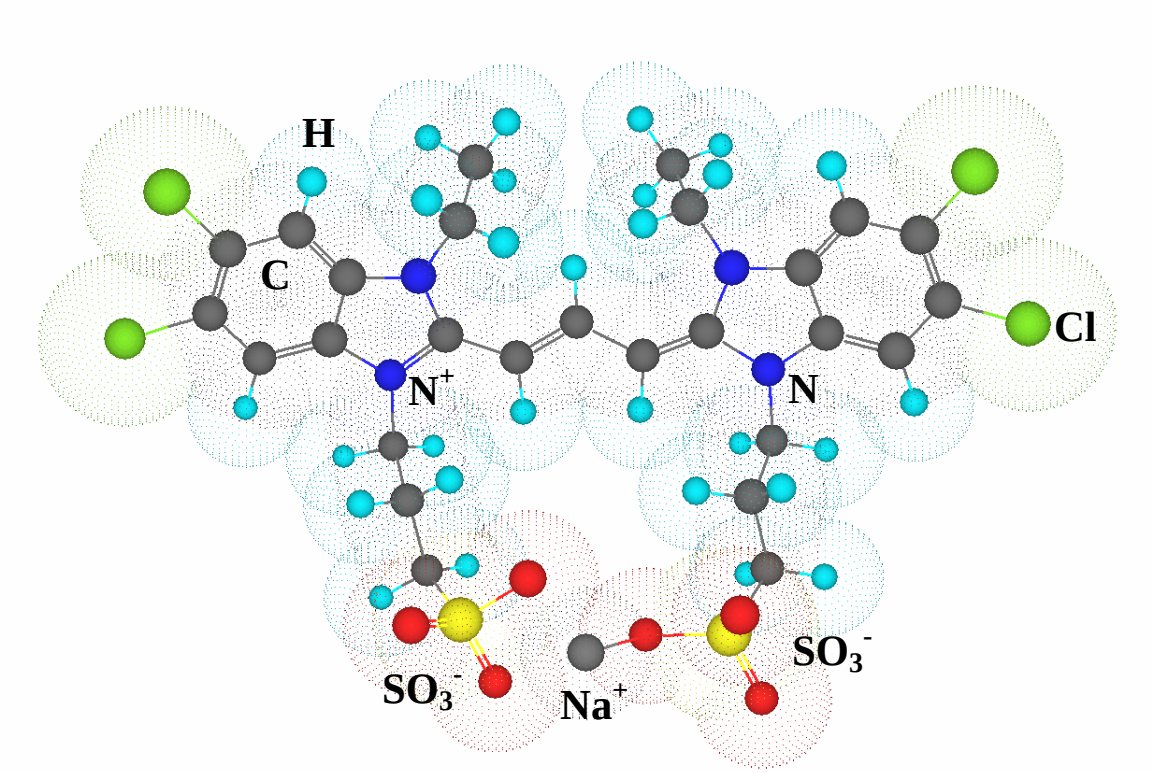

Figure I.2 Diagram of TDBC, a J-aggregating cyanine dye used throughout this project.

The LBL deposition method and the dye TDBC are used extensively throughout the rest of this thesis in developing the methods for analysis, patterning, and deposition of highly absorptive thin films and applying those methods to thin films of J-aggregates.

II. Properties of Layer-by-Layer J-Aggregate Thin Films Grown on Glass

This section describes research in the analysis of the properties of highly absorptive thin films, specifically using LBL J-aggregate thin films formed on glass substrates. The optical and morphological properties of LBL J-aggregate thin films make them well-suited for applications that utilize the strong coupling of light and matter.

II.A. Procedure for Creating Samples for Analysis

Thin films of TDBC J-aggregates grown on glass are used to probe optical and morphological properties. Figure II.1 shows a schematic of the sample structure and molecular diagrams of the thin film constituents. An LBL process is used to prepare the samples; glass substrates are immersed in cationic PDAC and anionic TDBC, a J-aggregate forming cyanine dye. Samples with different numbers of PDAC/TDBC layers are produced in order to observe the thin film structure at various stages of growth using atomic force microscopy (AFM). Figure II.2 shows AFM images throughout the various stages of growth with histograms showing formation of PDAC/TDBC layers and a plot of RMS roughness versus the number of SICAS.

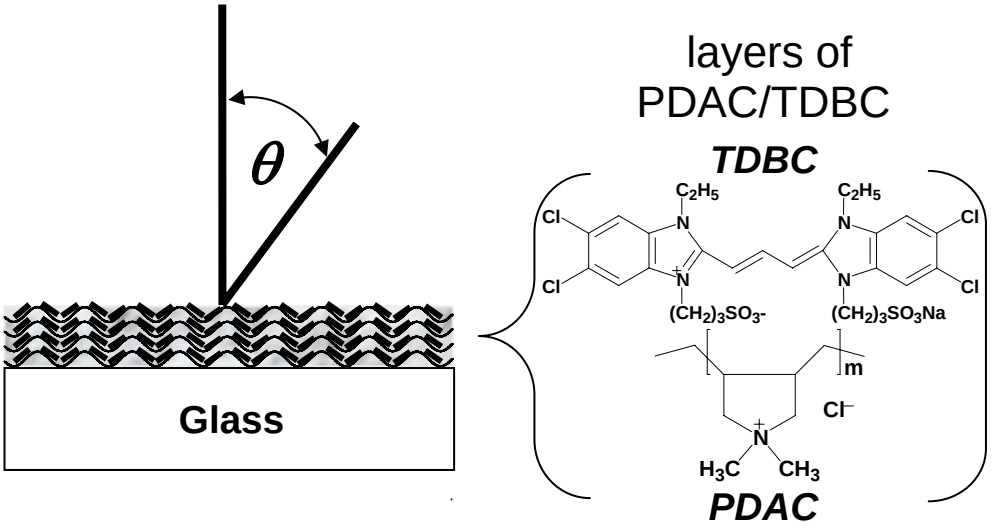

Figure II.1 Layer constituents and sample structure. The polycation used in the LBL growth is PDAC, and the anion is TDBC, a J-aggregate-forming cyanine dye. Optical measurements are taken with the LBL-film side of the sample facing the light beam at a specified angle θ away from the normal.

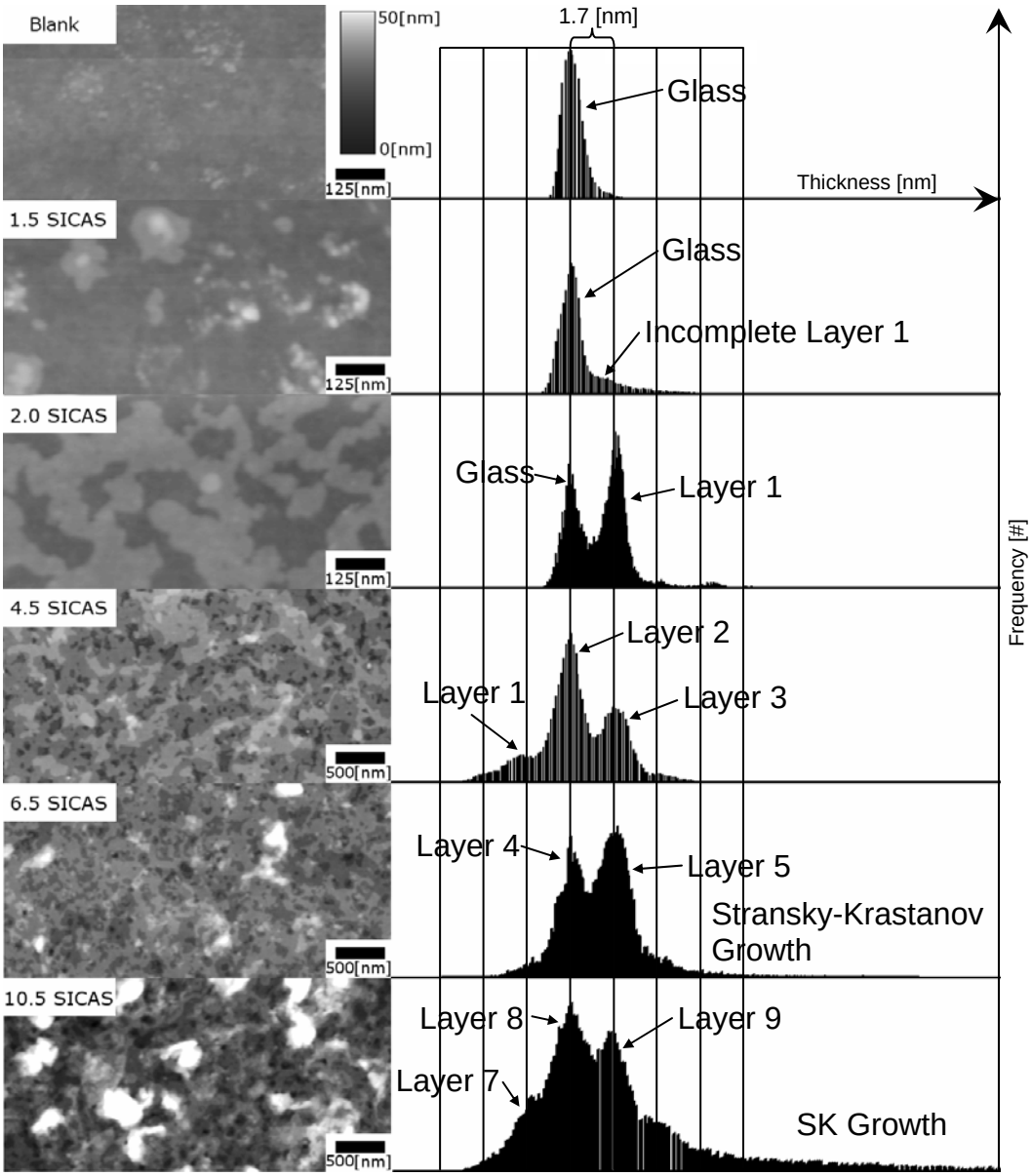
Blank
50[nm]
0[nm]
125[nm]
1.7 [nm]
Glass
Thickness [nm]
1.5 SICAS
Glass
Incomplete Layer 1
125[nm]
2.0 SICAS
Glass
Layer 1
125[nm]
4.5 SICAS
Layer 2
Layer 1
Layer 3
500[nm]
6.5 SICAS
Layer 4
Layer 5
Stransky-Krastanov
Growth
500[nm]
10.5 SICAS
Layer 8
Layer 9
Layer 7
SK Growth
500[nm]
Frequency [#]

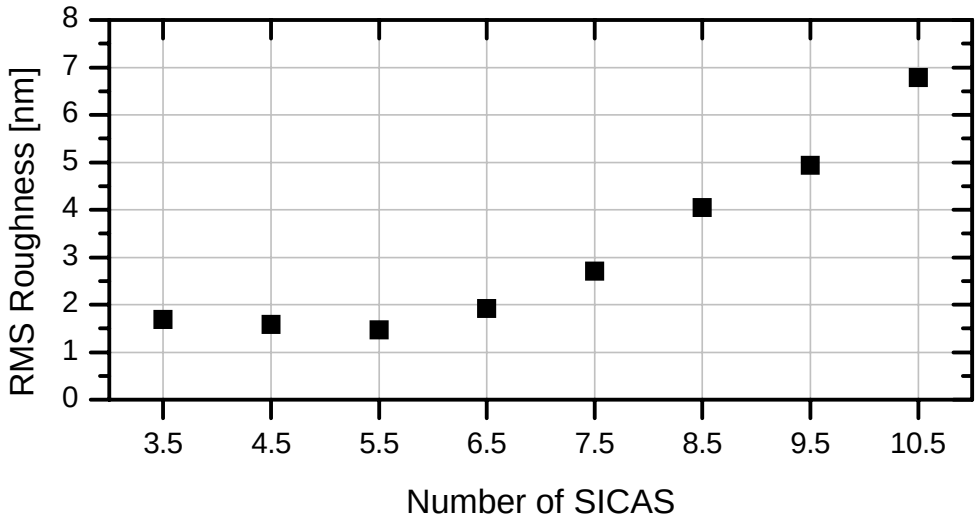
RMS Roughness [nm]
0
1
2
3
4
5
6
7
8
3.5
4.5
5.5
6.5
7.5
8.5
9.5
10.5
Number of SICAS

Figure II.2 Atomic force microscope (AFM) images of LBL J-aggregate growth with histograms of thickness frequency. Each SICAS consists of a PDAC adsorption step followed by a TDBC adsorption step, with N.5 SICAS referring to N SICAS followed by an additional PDAC adsorption step. The AFM images show samples that underwent the indicated number of SICAS. The top three images show that significant PDAC/TDBC layered growth is not evident until 2.0 SICAS. The bottom three images show the build-up of thick layers. The histograms are lined up at the dominant film thicknesses to show that each layer is about 1.7 nm thick, the estimate used when modeling the optical constants of the films. The histograms are created from the full 1 um^2 and 16 um^2 images for the first three and last three films shown, respectively. The layer numbers indicated in the histograms are based on the progression of layer growth observed in AFM images. The plot shows the roughness profile of films from 3.5 to 10.5 SICAS. The roughness is nearly constant until 6.5 SICAS, when the dominant growth regime changes from layered to Stransky-Krastanov (SK) type. All images have a vertical scale of 50 nm.

As shown in the AFM images for 1.5 SICAS and 2.0 SICAS compared to blank glass, the layered structure of the PDAC/TDBC J-aggregate films does not appear until the second dye immersion. This delay is likely caused by the lack of a precursor layer or surface treatment on the glass support. The images show that layered growth is still dominant at 4.5 SICAS, but at 6.5 SICAS and 10.5 SICAS the growth has shifted to a Stransky-Krastanov (SK) type of process, forming large islands of material. To quantify the growth trend, RMS roughness is measured from 16 um^2 AFM images of films that underwent 3.5 SICAS to 10.5 SICAS. The plot in Figure 2 shows that a mostly constant

RMS roughness in the range of 1.4 to 2.0 nm persists through the first 5.5 SICAS, indicating layered growth, but beyond 6.5 SICAS, the roughness increases, indicating the shift to SK-type growth.

II.B Analysis of Optical Properties

The thickness data obtained from the AFM measurements are combined with optical transmittance and reflectance data to extract the optical constants of the LBL PDAC/TDBC J-aggregate films. Figure II.3 plots measured optical data and results of the analysis.

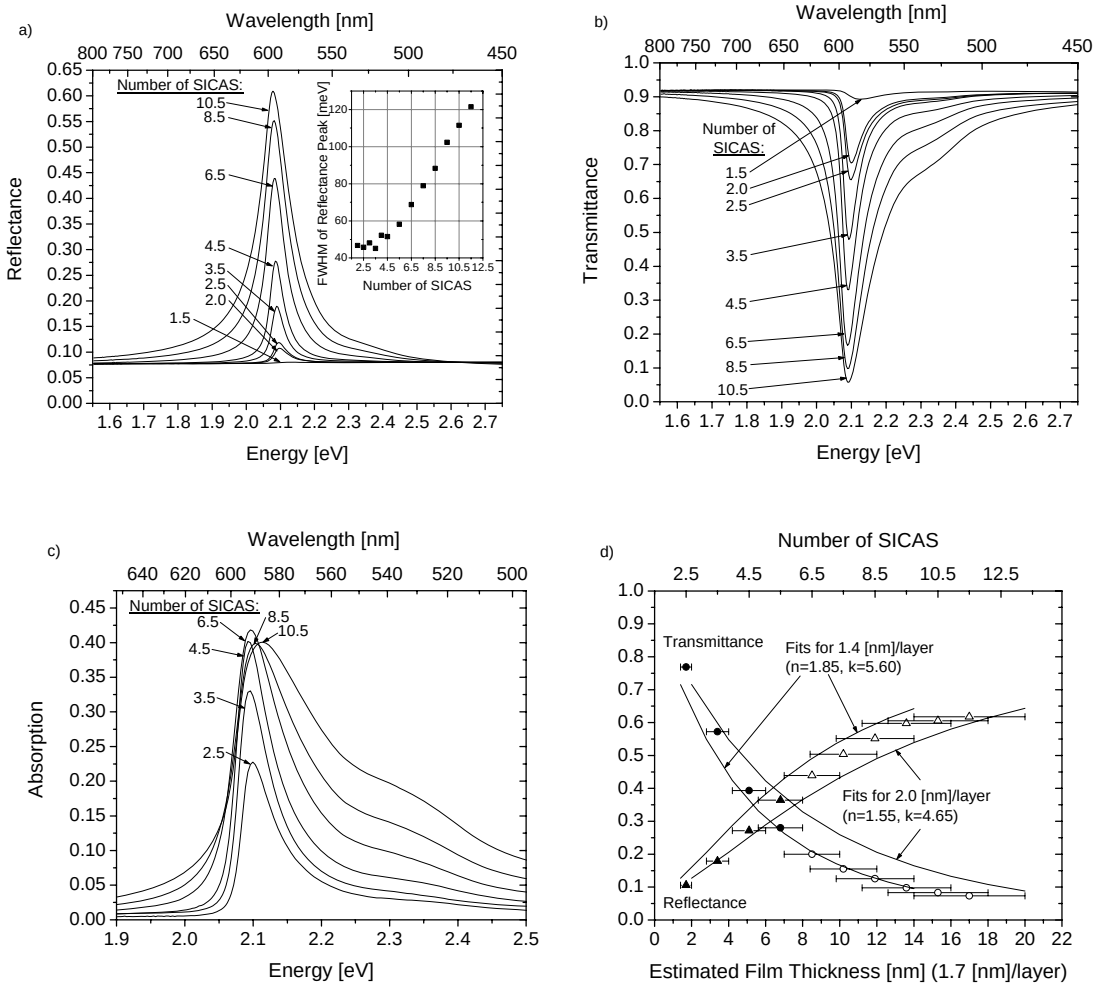

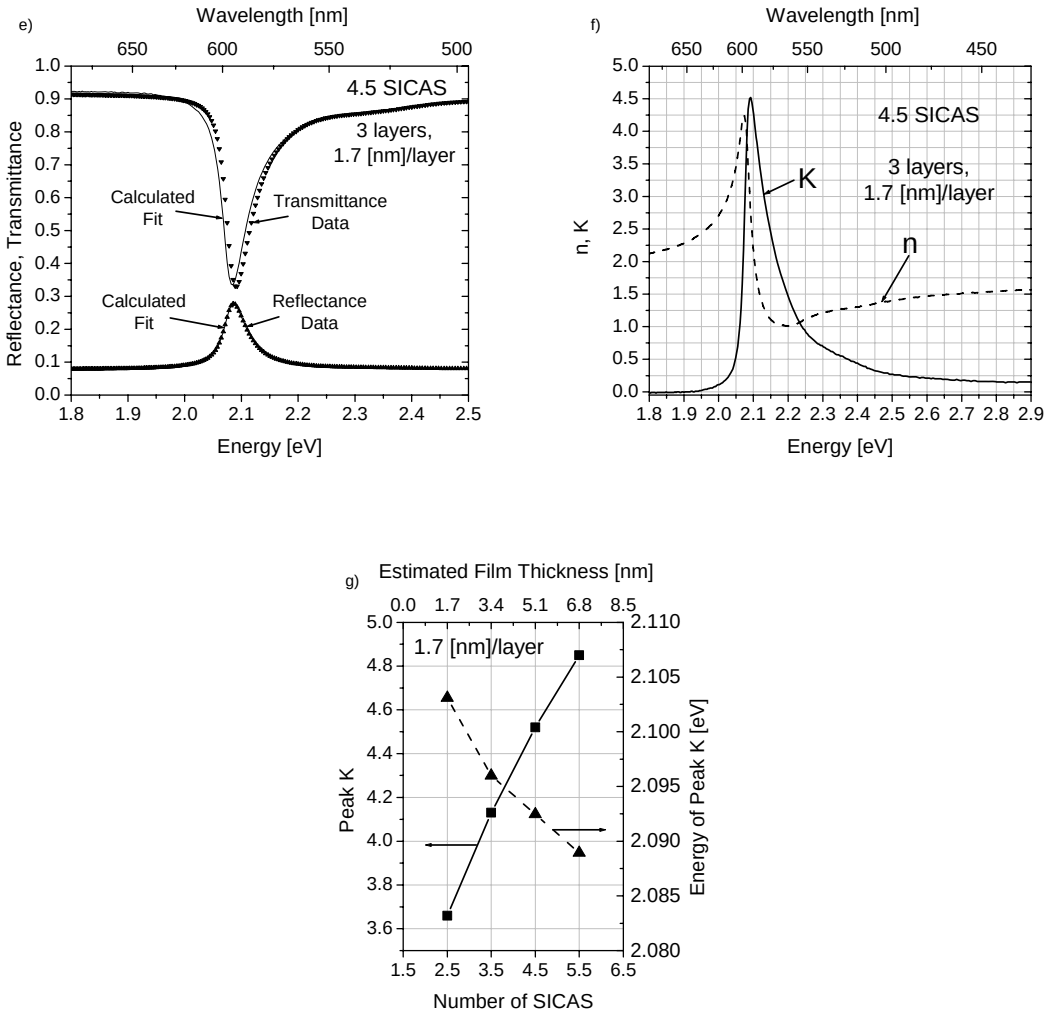

Figure II.3 Optical data and characterization of optical properties for LBL PDAC/TDBC J-aggregate films. Plots (a) and (b) show reflectance, R, at θ=7° and transmittance, T, at θ=0° for a series of samples that underwent different numbers of SICAS. Plot (a, inset) shows the FWHM of the reflectance peak as a function of number of SICAS. Plot (c) shows absorption for the same samples given by 1-R-T. Plot (d) shows the transmittance and reflectance data at wavelength λ=596 nm plotted versus film thickness, along with fits from our model. The fits are based exclusively on the first four (filled) data points where layered growth is the dominant mode of film formation. Consequently, for thicker

films (outlined data points) where SK-type growth is dominant, the thickness shown along the x-axis is to be interpreted as the AFM-determined thickness estimate for the layered portion, not the SK portion, of the film. The two fits plotted show the range in the complex index of refraction. Plot (e) shows measured reflectance and transmittance for 4.5 SICAS (5.1 nm thick film, 3 layers with 1.7 nm per layer) and calculated spectra using the (n,K) shown in Plot (f). Plot (f) shows (n,K) for the 4.5 SICAS film in (e) obtained through a Kramers-Kronig (KK) regression based on reflectance data. Plot (g) shows the range of the peak in k for 2.5 SICAS to 5.5 SICAS films from KK regression as well as the position of the peak in k versus energy, assuming a thickness of 1.7 nm per layer.

Light propagation through the sample is modeled by using propagation and interface matching matrices, with film thicknesses as inputs to the model and refractive indices as fitting parameters. The implementation details of this model are described further in the experimental section in Appendix A. Figure II.4 shows an outline of the propagation and matching matrix model, including the relevant equations.

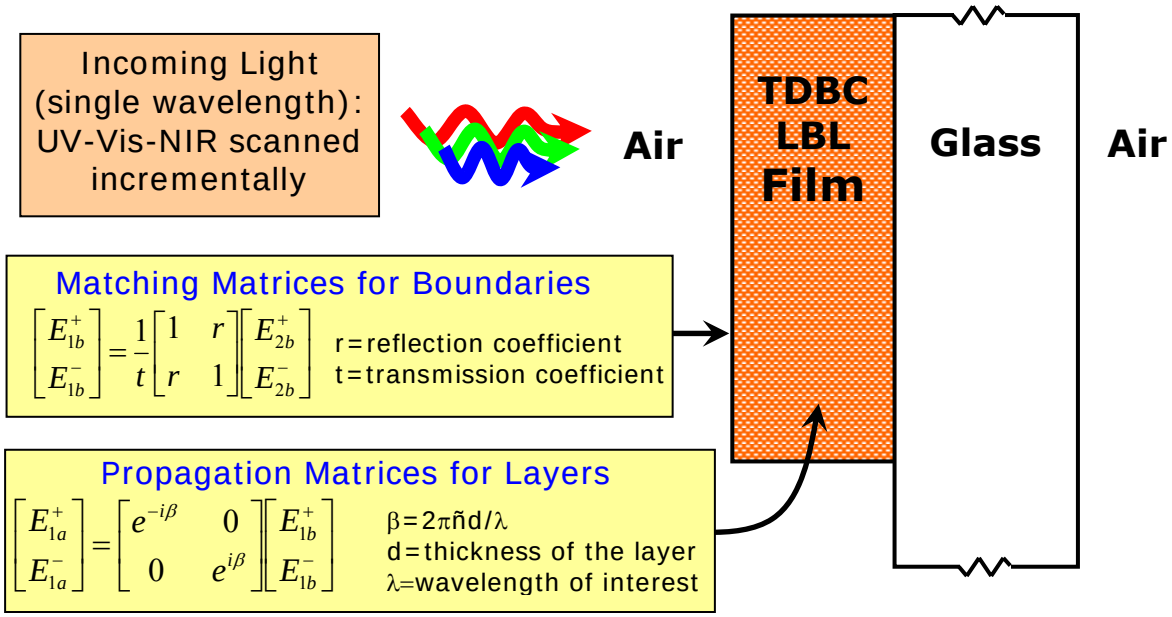

Figure II.4 Outline of the propagation and matching matrix model used in analyzing the thin film samples. Reflectance and transmittance measurements are made using a spectrometer which can sense light at ultraviolet, visible, and near infrared wavelengths (UV-Vis-NIR). Each boundary and layer in the light's path is modeled using the appropriate matrix, leaving the thin film's index of refraction as the missing parameter to be found using numerical regression (film thickness is from AFM measurements).

Two methods are employed in calculating the (n,K) values. In the first method, the (n,K) values are obtained by minimizing the sum of least-squared errors of the calculated transmittance and reflectance for the first four sample thicknesses. This approach is similar to that described by Djurišić *et al.*, however in this method a single (n,K) fit is performed, and the use of a penalty function in calculating the least-squared errors is not incorporated.[4] In the first method, the absorption constant in the layered growth regime is assumed constant as more PDAC/TDBC layers are deposited. The ranges in n and K values are [0.05,5] and [0,6], respectively, with a resolution of 0.05 in

both. It should be noted that since no PDAC/TDBC layer is evident for the first 1.5 SICAS, the transmittance and reflectance data for the first layer correspond to what we refer to as the 2.5 SICAS sample. Numerical fits to the thickness-dependent reflectance and transmittance data at wavelength λ=596 nm based on the first method are shown in Figure II.3(d) for complex index of refraction with a real part, n, between 1.55 and 1.85 and an imaginary part, K, between 4.65 and 5.60. The high extinction coefficient, K, corresponds to an absorption constant of the film of $\alpha=4\pi K(\lambda)/\lambda=(1.05 \pm 0.1) \times 10^6$ cm^{-1} at λ=596 nm. In our analysis, complete layer coverage is assumed in contrast to the partial coverage observed in Figure II.2. This assumption underestimates the K values for the thin film.

The second method employed in calculating the (n,K) values is based on the Kramers-Kronig (KK) transformations, which relate the real and imaginary parts of the index of refraction. The details of the KK regression are explained in Appendix A. For samples that underwent 2.5 SICAS (estimated as 1 complete layer) to 5.5 SICAS (estimated as 4 complete layers), the (n,K) spectra for each sample are calculated from the sample's reflectance spectrum. Figures II.3(e) through II.3(g) show the results of the KK regressions. Figure II.3(e) shows the measured transmittance and reflectance for the 3 layer (5.1 nm thick) film along with the reflectance and transmittance calculated from the (n,K) spectra in Figure II.3(f). The transmittance calculated from the KK regression is in good agreement with the measured transmittance. Figure II.3(g) shows the peak in K for 1 layer (1.7 nm thick) to 4 layer (6.8 nm thick) films calculated using the KK regressions as well as the movement of the peak in K to lower energies as the number of

layers increases. The results of the KK regression confirm the high magnitude of the absorption constant of the film found through the first method.

II.C Results and Discussion

Several trends are noticeable in the optical data as samples undergo more SICAS. The reflectance data in Figure II.3(a) show that the peak in reflectance moves to lower energy and the full-width at half maximum (FWHM) increases. In addition, Figure II.3(c) shows the onset of a high energy peak in absorption. Lastly, the KK regression results plotted in Figure II.3(g) show the peak K value increasing with the number of SICAS. Two approaches have been considered in explaining these trends.

The first explanation is based on the changing morphology of the thin films. The assumption of complete layer coverage in numerical analysis could be responsible for the apparent increase in K plotted in Figure II.3(g). In addition, the increase in reflectance FWHM may be due to a weak microcavity caused by SK growth or increasing inhomogeneous broadening. Lastly, the onset of the high energy peak could be attributed to vibronic states in the J-aggregate, as noted in previous studies of J-aggregate monolayer films deposited using a Langmuir-Blodgett technique.[24,25]

An alternative explanation is based on strong coupling of the J-aggregate excitons to the electromagnetic field in the form of exciton-polaritons.[26-30] The effects of strong coupling will be more pronounced as the density of dipoles increases, resulting in a higher K for the films as more layers are added. Additionally, a larger reflectance FWHM will result from an increase in the splitting between the exciton-polariton longitudinal and transverse modes. Lastly, the high energy peak in absorption could be attributed to the exciton-polariton longitudinal mode. The observed trend in Figure

II.3(a) of the peak in reflectance moving to lower energy is consistent with both explanations. A weak cavity effect due to SK growth may be responsible for the small shift in the peak reflectance to lower energy as the cavity thickness increases.

The described analysis of LBL J-aggregate thin films shows how to use optical and morphological measurements of highly absorptive thin films to determine the complex index of refraction, an important parameter in the design of photonic devices.

III. General Deposition and Patterning Techniques for LBL J-Aggregate Thin Films

As shown in the previous section, highly absorptive thin films, like those of J-aggregates, have remarkable properties that make them well-suited for applications which utilize the strong coupling of light and matter. In order for this new class of photonic devices to be realized, however, processes for patterning and deposition must be developed for the highly absorptive thin films at the heart of the new devices. Even simple patterns like those shown in Figure III.1 can be difficult to produce, especially when the patterned film must be placed in a complex device structure. Microcontact printing (μCP), a stamping process, provides a solution to the processing and deposition dilemma for highly absorptive thin films like those of J-aggregates. Patterns from the mundane, like those in Figure III.1, to the complex can be produced, and such patterns can be made even in complex device structures which include fragile materials.

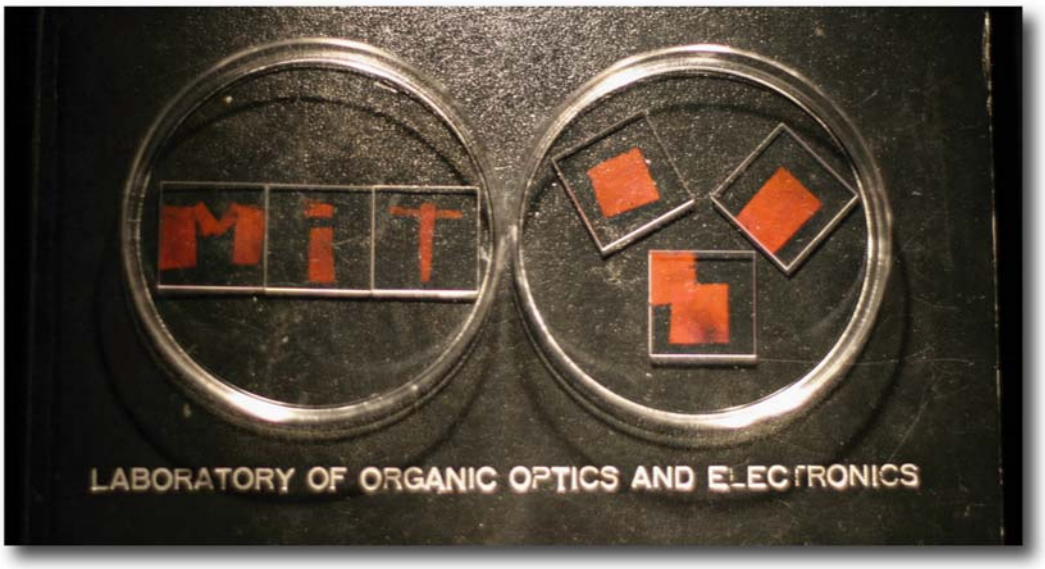

Figure III.1 Patterned J-aggregate thin films on glass, formed and deposited through a microcontact printing (μCP) process.

III.A. Microcontact Printing

To date, J-aggregate deposition methods, such as LBL deposition, spin-casting in a polymer matrix, and Langmuir-Blodgett have required film deposition in a solvent environment.[12-14] The exposure of a J-aggregate optoelectronic device in fabrication to solvents can potentially damage other constituent optical or electrical active materials and restrict device fabrication steps. In this section, a J-aggregate thin film patterning and deposition method that eliminates solvents from the final deposition steps is demonstrated.

With LBL deposition of J-aggregates, thin films of J-aggregates are formed on an elastomer stamp, and using soft lithography, the films are stamp-transferred onto a substrate with appropriate surface chemistry.[31,32] Two LBL methods that can be used to grow thin films of J-aggregates on PDMS (polydimethylsiloxane) elastomer stamps are presented. In both methods, the J-aggregating cyanine dye is the anion TDBC. The

choice of LBL method depends on whether a strong or weak polyelectrolyte is used as the polycation along with the anionic TDBC. In Method 1, the strong polycation PDAC is used, and an LBL deposition sequence similar to that previously described for J-aggregate thin films grown on glass is followed.[33] Additionally, in Method 1, the PDMS is treated with the strong polyanion PSS (poly(sodium-4-styrenesulfonate)) prior to undergoing sequential immersions in cationic and anionic solutions (SICAS) of PDAC/TDBC. In Method 2, the weak polycation PAH (poly(allylamine hydrochloride)) is used, and PDMS pretreatment is omitted. The structural formulas of the materials used in both methods are summarized in Figure III.2(a). Detailed descriptions of both methods are provided in the experimental section in Appendix B.

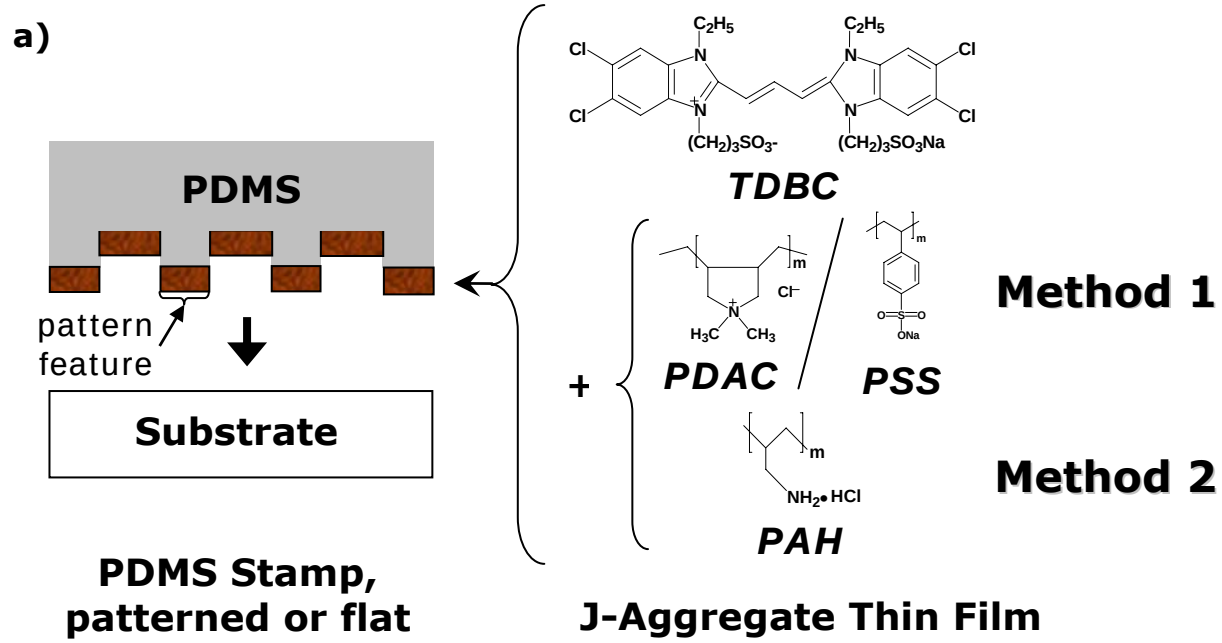

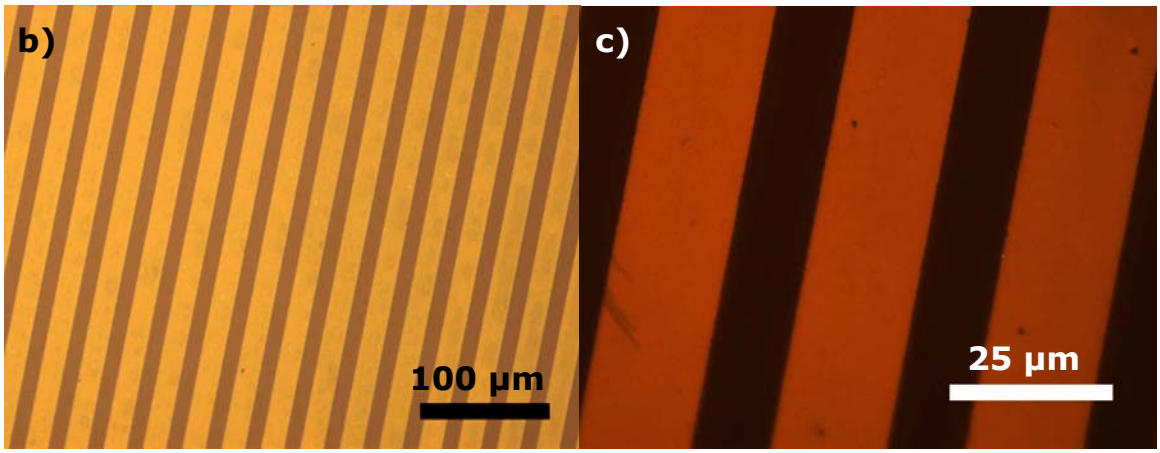

Figure III.2 (a) Soft lithography schematic and structural formulas of J-aggregate thin film constituents. The stamps are either flat or, for soft lithography, patterned PDMS. Patterned PDMS stamps are created by curing PDMS on silicon molds. J-aggregate thin films are created in a layer-by-layer (LBL) process in which substrates undergo sequential immersions in cationic and anionic solutions (SICAS). The J-aggregating cyanine dye is TDBC, an anionic dye. In Method 1, PDMS is pretreated in a process involving the polyanion PSS, and PDAC is used with TDBC to create the J-aggregate thin film. In Method 2, PAH is directly substituted for PDAC in the J-aggregate thin film, and no stamp pretreatment is performed. Optical microscope images of a patterned J-aggregate LBL thin film transferred onto glass are shown in (b) and (c). (b) A patterned, 3 SICAS PAH/TDBC film transferred from a patterned PDMS stamp is shown in a reflectance mode image. (c) The same 3 SICAS patterned film is shown in photoluminescence with green light excitation, revealing sub-micron roughness in pattern definition.

PDAC/TDBC thin films are not stable when grown directly on untreated PDMS. To address the issue of stable J-aggregate thin film growth on PDMS, the two methods

introduced above were developed. To increase film stability in Method 1, the PDMS stamps are first treated with oxygen plasma to form a glass-like layer on the surface of the PDMS.[34] The stamps are then dipped in a strongly basic solution, pH 14 sodium hydroxide in deionized (DI) water, to give a strong negative charge to the surface layer.[34,35] Finally, the stamps undergo 2 SICAS of PDAC/PSS in order to form a thin polyelectrolyte LBL film that supports the J-aggregate overlayers. J-aggregate thin films of varying numbers of SICAS of PDAC/TDBC are then grown.

Previous work on the multilayer transfer printing of polyelectrolyte thin films demonstrated that PAH can adsorb to PDMS readily via hydrophobic interactions under the right pH conditions.[32] In Method 2, a weak polycation PAH is substituted for PDAC in the LBL J-aggregate thin film growth process, and varying number of SICAS of PAH/TDBC are grown directly on the PDMS stamps with no pretreatment steps necessary.

III.B Results and Discussion

The stamps are dried using a stream of nitrogen gas after LBL growth is complete, and the J-aggregate thin films are then transferred through stamping to clean, oxygen-plasma-treated glass slides for analysis. Near-normal spectral reflectance at $\theta=7°$ and transmittance at $\theta=0°$ are measured, where θ is the angle away from the surface normal. Atomic force microscopy (AFM) measurements are performed to determine film thickness. The films are manually scratched, and the step height is profiled. The complex indices of refraction ($\tilde{n}=n+iK$) for the stamped LBL J-aggregate thin films are determined by fitting these data with the regression method described in Appendix A,

based on Kramers-Kronig (KK) relations and a thin film dielectric model using propagation and matching matrices.[33,36]

Figure III.3 summarizes the measurements and results of KK regression on stamped PDAC/TDBC J-aggregate thin films (Method 1). Figure III.3(a) shows reflectance and transmittance data from stamped films grown with varying numbers of SICAS. Figure III.3(b) shows the measured thicknesses of the stamped films. Figure III.3(c) summarizes the results of KK regression, performed using transmittance data from the series of samples studied. Finally, Figure III.3(d) shows the index of refraction across the measured spectrum for one of the samples, a 5.5 SICAS PDAC/TDBC stamped film with a measured film thickness of 8.8 nm.

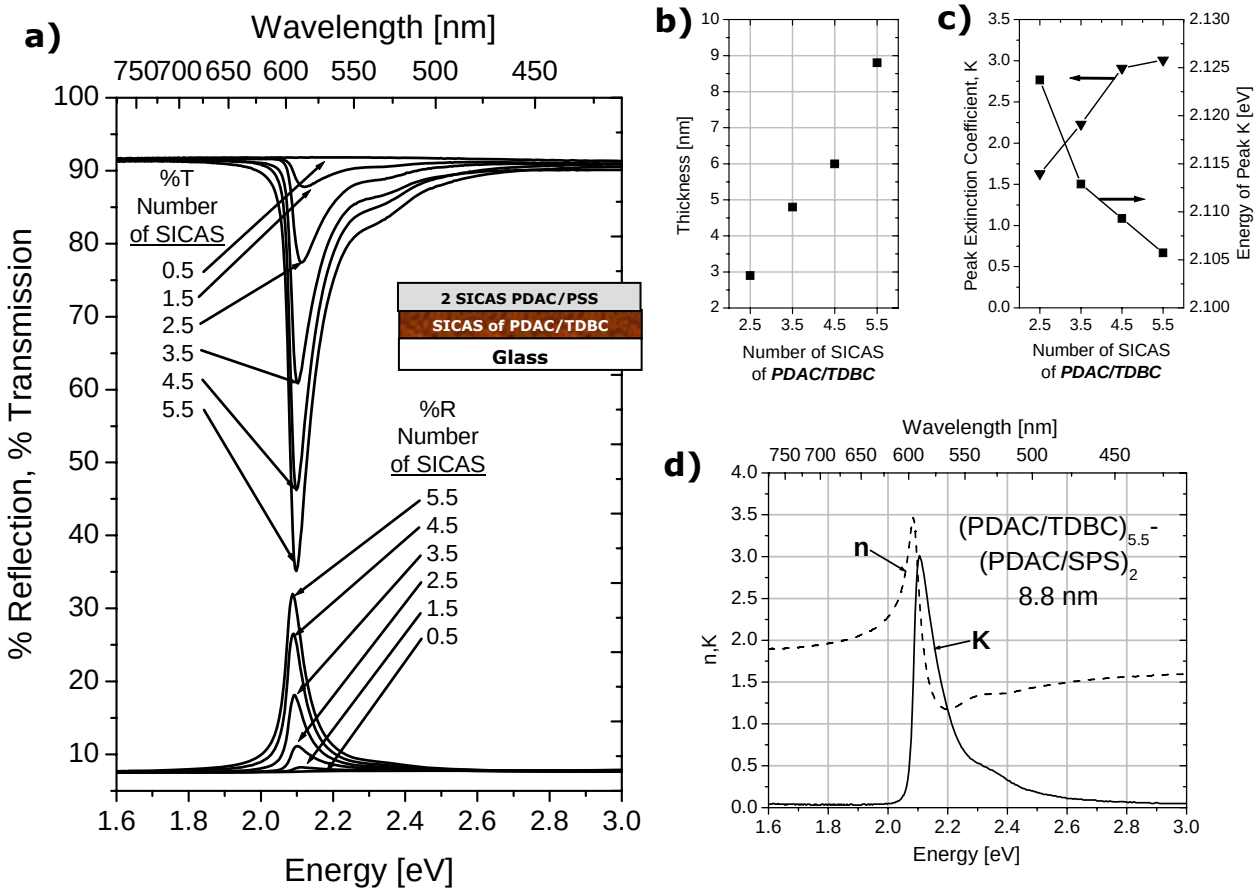

Figure III.3 Measurements and results of Kramers-Kronig (KK) regression for a series of stamped films on glass formed on PDMS using Method 1 (PDAC/TDBC). Plot (a) summarizes the reflectance and transmittance data for stamped films formed on PDMS using Method 1. Plot (b) shows AFM-derived thickness data from the films. Plot (c) shows the value and energy of the peak extinction coefficient derived using KK regression. Plot (d) shows the complex index of refraction ($\tilde{n}=n+iK$) of the 5.5 SICAS PDAC/TDBC stamped film.

It should be noted that reflectance data are generally used for KK regression, in part because transmittance measurements can be affected by scattering in the film. However, transmittance measurements are used here since the stamped films do not cover the entire glass substrate, and in the Cary 5E spectrometer used, transmittance measurements have a controllable spot size. This control allows one to avoid measuring the thicker film build-up that can sometimes occur at the edges of the stamps and can potentially affect reflectance measurements. Because the reflectances calculated from the KK-derived indices of refraction are at most 5 to 10% lower than the measured reflectances, the peak thin film absorption constant calculated is a lower bound. If the derived indices of refraction were significantly affected by scattering measured in transmittance, the opposite would be the case, and the calculated reflectances would be higher than those measured.

Using the results of the KK regressions, the peak linear thin film absorption constant can be calculated from the peak in the extinction coefficient, the imaginary part of the index of refraction, using the formula $\alpha=4\pi K(\lambda)/\lambda$, where K is the extinction

coefficient and λ is the wavelength of interest in centimeters. For the 5.5 SICAS PDAC/TDBC (Method 1) film shown in Figure III.3(d), the peak extinction coefficient is K=3.01 at λ=590 nm, which corresponds to a linear absorption constant of 6.4×10^5 cm^{-1}. This value is about 2/3 of that reported previously for a PDAC/TDBC film grown on glass.[33] However, because this film may include the PDAC/PSS pretreatment, the overall density of dye in the final film is likely reduced.

The same analysis is performed on stamped PAH/TDBC films (Method 2). Figure III.4 summarizes the measurements and results of KK regression. Figure III.4(a) shows reflectance and transmittance data for varying numbers of SICAS. Figure III.4(b) shows the measured thicknesses of the stamped films. Figure III.4(c) summarizes the results of KK regressions using the transmittance data. Figure III.4(d) shows the index of refraction for a 3 SICAS PAH/TDBC stamped film with a measured film thickness of 7.6 nm.

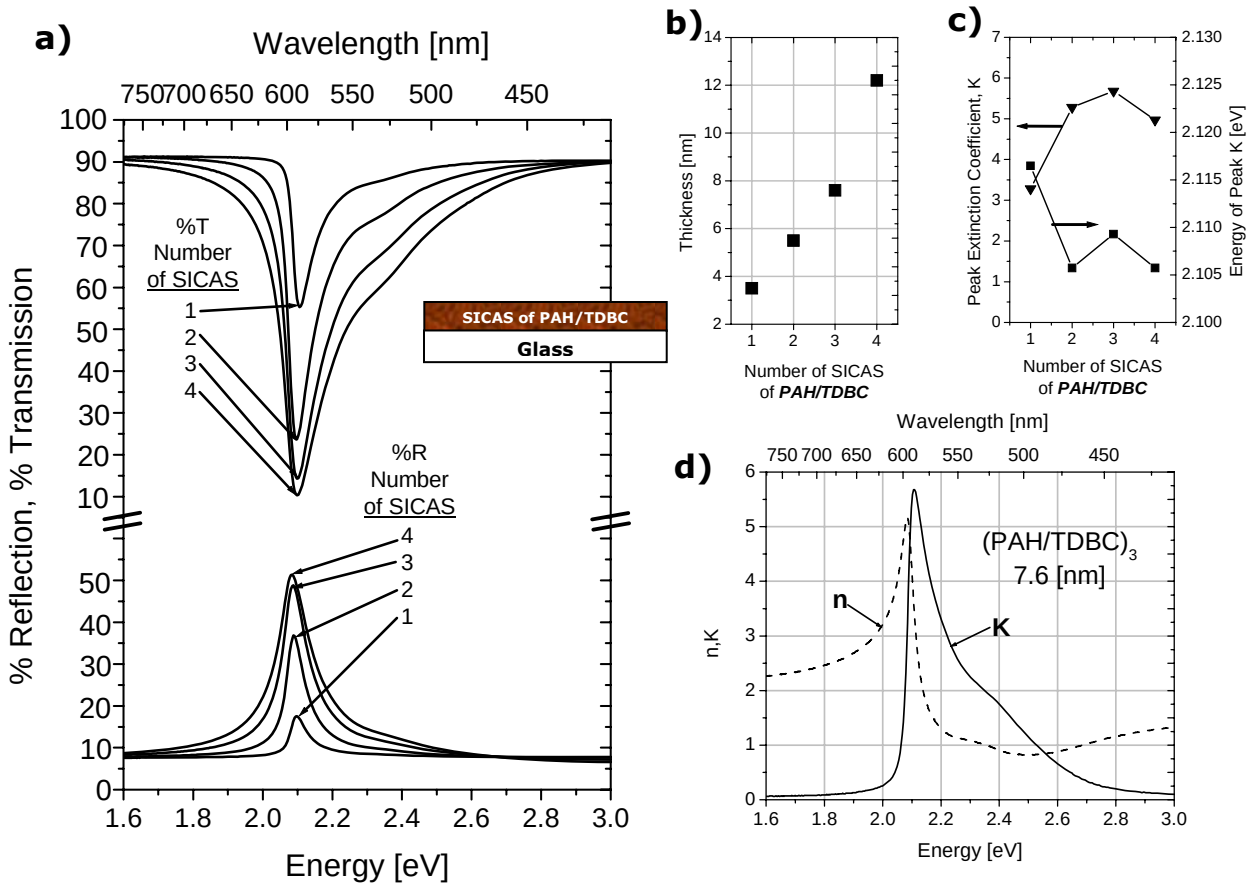

Figure III.4 Measurements and results of KK regression for a series of stamped films on glass formed on PDMS using Method 2 (PAH/TDBC). Plot (a) summarizes the reflectance and transmittance data for stamped films. Due to overlap of measurements in Plot (a), the reflectance and transmittance data have been offset. Plot (b) shows the AFM-derived thickness data from the films. Plot (c) shows the value and energy of the peak extinction coefficient derived using KK regression. Plot (d) shows the complex index of refraction of the 3 SICAS PAH/TDBC stamped film.

The peak extinction coefficient of the 3 SICAS PAH/TDBC (Method 2) film shown in Figure III.4(d) is K=5.68 at λ=589 nm, which corresponds to a linear absorption

constant of 1.2 x 10^6 cm^{-1}. The high linear absorption constant indicates a high density of dye in the film, which is likely due in part to the ability of PAH versus PDAC to adsorb to the PDMS stamp. The smaller size of the PAH monomer compared to the PDAC monomer may also contribute to a higher dye density in the film due to a higher density of adsorption sites. Finally, the PAH/TDBC films do not have the additional material from PDMS pretreatment that may also be present in stamped films grown with Method 1.

As suggested in Figure III.2(a), in addition to decoupling J-aggregate thin film formation and deposition, stamping allows for the use of soft lithography. Soft lithography using PDMS and thin films was first introduced in the 1990s, and its use in patterning LBL stamped thin films was also discussed in the LBL multilayer transfer printing study referenced earlier.[32,37-43] J-aggregate LBL thin films are patterned by growing the films on PDMS stamps molded with a silicon master. The films are then stamped, and only the J-aggregate thin film portions on the raised PDMS surfaces are transferred. Figures III.2(b) and III.2(c) show images of a patterned J-aggregate thin film, initially formed on PDMS using Method 2, and stamped onto glass. This form of patterning J-aggregate thin films does not require the J-aggregates to be exposed to any reactive etch process.

IV. Conclusion

The optical and morphological analysis methods demonstrated in Section II show that LBL assembled thin films of PDAC/TDBC J-aggregates possess remarkable morphological and optical properties that make them well-suited for use in strong coupling optoelectronic applications, enabling the creation of exciton-polariton optoelectronic devices that operate at room-temperature.[6,7] With LBL, J-aggregates

form nanometer-scale physical layers, allowing highly absorbing thin films to be assembled with precision thickness control. Moreover, the high absorption constant of the PDAC/TDBC films grown on glass, $\alpha=(1.05 \pm 0.1) \times 10^6$ cm^{-1} at $\lambda=596$ nm, is a lower limit, as even higher absorption constant values could be obtained by developing full coverage of the substrate surface with similarly directed J-aggregate domains.

Additionally, the patterning and deposition methods demonstrated in Section III indicate that stamped LBL J-aggregate thin films have many of the same remarkable characteristics as the LBL J-aggregate thin films grown on glass. Using the two methods for growing films described, J-aggregate thin films with high thin film absorption constants can be stamped without exposing the substrate to significant moisture or immersing the substrate in the solvents used in forming the J-aggregate thin films. This decoupling of the formation of J-aggregate thin films from their formation could enable the use of J-aggregates in a wider set of organic and inorganic devices. Additionally, stamping J-aggregate thin films using PDMS allows for the use of soft lithography, which has the potential of allowing for patterned photonic devices based on J-aggregates as well as for large-area integration of photonic devices using J-aggregates as an active material. Lastly, by tuning the surface chemistry of the stamp surface, other methods of J-aggregate thin film formation on the stamp, such as Langmuir-Blodgett, could potentially be used, allowing for stamping of an even wider variety of thin films of J-aggregating dyes.

Together, the analysis, patterning, and deposition methods for highly absorptive thin films detailed in this thesis and applied to J-aggregates help to further the formation

of an entirely new class of photonic devices based on the strong coupling of light and matter by enabling both the design and manufacture of such devices.

V. Acknowledgements

First, I would like to acknowledge the financial support that made the research presented in this thesis possible. I am grateful to the National Defense Science and Engineering Graduate Fellowship program for its support. Additionally, this work was supported by DARPA Optocenter, MIT's NSF MRSEC Program, and the DARPA SPOT-ON Seed Grant.

Many of the measurements reported in this thesis were performed in the MIT Center for Material Science and Engineering Shared Analytical Facilities, and I would like to acknowledge the assistance of Libby Shaw for the excellent equipment training she provides and her hard work in maintaining such a useful lab.

I am grateful to Professor Michael Rubner for his informative discussions regarding polyelectrolyte LBL growth and encouragement to use PAH in growing J-aggregates—advice that was eventually followed and proved fruitful when trying to grow stable thin films on PDMS.

Also, I would like to acknowledge collaborators in Professor Arto Nurmikko's group at Brown University for their insightful discussions regarding J-aggregate physics. I have enjoyed the frequent video conferences with them and learned much from their expertise in time-resolved optical measurements.

None of this work would have been possible without the knowledge, insight, and persistence of Jonathan "Yaakov" Tischler, my colleague and predecessor who did the real hard work of getting this whole project started. His investigative spirit and sharp

mind led to our use TDBC and the LBL process, and his knowledge of physics has led us further down the path toward polaritonic devices. I've learned more physics from my discussions from Yaakov than in most of my previous classwork, and I hope some of his insight has rubbed off on me as well.

The support of my advisor, Professor Vladimir Bulović, has been instrumental in my success thus far. I would like to thank him specifically for aiding and abetting Yaakov's and my forays into materials science, which are, if not always fruitful, certainly enjoyable and enlightening.

Lastly, it goes without saying that I would not even have had the chance to write any Master's thesis were it not for the support of my family and of my girlfriend, Corinne Packard. I am thankful for my family's continual support, for my parents' sacrifice in sending me to MIT in the first place—it certainly wasn't cheap—and for entrusting me with so many of their hard-earned financial resources to further my education. And without the support and encouragement of Corinne, I certainly would not have achieved the success I enjoy today. It's been fun, and I look forward to further adventures in research in the coming years!

Appendix A. Experimental Details for Section II

J-aggregate thin films were produced using layer-by-layer assembly. Layers of polyelectrolyte and J-aggregate-forming dye were alternately adsorbed onto glass slides. The dye used was 5,6-dichloro-2-[3-[5,6-dichloro-1-ethyl-3-(3-sulfopropyl)-2(3H)-benzimidazolidene]-1-propenyl]-1-ethyl-3-(3-sulfopropyl) benzimidazolium hydroxide, inner salt, sodium salt obtained from Nippon Kankoh Shikiso Kenkyusho Co., Ltd. (CAS 28272-54-0). The polyelectrolyte used was poly(diallyldimethylammonium chloride), 20% by weight in water, M_w=400,000-500,000, obtained from Sigma-Aldrich (CAS 26062-79-3). The dye solvent and rinses for the dye adsorption step were approximately pH 9 solutions of deionized (DI) water plus sodium hydroxide. The effect of pH on TDBC has been documented.[44] The sodium hydroxide was obtained from EM Science. The polyelectrolyte solvent and rinses for the polyelectrolyte adsorption step were DI water.

A standardized routine was used to prepare the dye and polyelectrolyte solutions. The dye solution was approximately $5x10^{-5}$ M. Once the dye was added to the dye solvent, the dye bucket was placed in an ultrasonic cleaner to sonicate for 30 minutes. The dye was then mixed with a one-inch magnetic spin bar for 10 minutes, sonicated for 20 minutes, mixed for 5 minutes, and finally sonicated for 5 minutes. The polyelectrolyte solution was approximately $3x10^{-2}$ M, prepared by adding 10 mL of polyelectrolyte to 390 mL of DI water. The polyelectrolyte solution was prepared using the same time intervals for mixing/sonication as the dye solution preparation, except sonication and mixing at each step were swapped. Care was taken throughout the deposition to shield the dye solution and samples from light.

Prior to the deposition, the glass slides were cleaned with a detergent solution (Micro-90), acetone, and isopropanol. The acetone, isopropanol, and methanol used in this study were OmniSolv-brand solvents made by EMD Chemicals. The slides were then treated with oxygen plasma for six minutes in a Plasma Preen system. The layer-by-layer deposition was performed using an automated Leica Autostainer XL. The polyelectrolyte adsorption step consisted of dipping the slides in polyelectrolyte solution for 15 minutes and in the three rinses for two minutes, two minutes, and one minute, respectively. The dye adsorption step used the same time intervals as those used in the polyelectrolyte adsorption step.

Upon removal from the stainer, each sample was blown dry using nitrogen gas. For each sample, the sample face that was not treated with oxygen plasma prior to deposition was cleaned using methanol to remove deposited layers.

Measurements for this study were performed in the MIT Center for Materials Science and Engineering Shared Analytical Lab. The atomic force microscopy (AFM) data were collected on a Digital Instruments D3000 Scanning Probe Microscope in tapping mode using phosphorus-doped silicon tips from Veeco. The optical data were collected using a Cary 5E UV-Vis-NIR spectrophotometer. The transmission data were collected with the light beam at normal incidence, $\theta=0°$. The reflectance data were collected in a V-W setup with the light beam incidence at $\theta=7°$ using the Cary Specular Reflectance Accessory in Absolute Reflectivity mode.

For numerical calculations, we modeled the films using propagation and matching matrices:[45]

$$\begin{bmatrix} E_{1a}^{+} \\ E_{1a}^{-} \end{bmatrix} = \begin{bmatrix} e^{-i\beta} & 0 \\ 0 & e^{i\beta} \end{bmatrix} \begin{bmatrix} E_{1b}^{+} \\ E_{1b}^{-} \end{bmatrix} \quad \text{(Eq. A.1)} \qquad \begin{bmatrix} E_{1b}^{+} \\ E_{1b}^{-} \end{bmatrix} = \frac{1}{t} \begin{bmatrix} 1 & r \\ r & 1 \end{bmatrix} \begin{bmatrix} E_{2b}^{+} \\ E_{2b}^{-} \end{bmatrix} \quad \text{(Eq. A.2)}$$

Eq. A.1 shows a propagation matrix equation, which relates the forward and reverse traveling electric field amplitudes at boundary (a) to the amplitudes at boundary (b). The medium (1) is modeled by the parameter $\beta=2\pi\tilde{n}d/\lambda$, where $\tilde{n}$ is the complex index of refraction of the medium, $\tilde{n}=n+iK$, and d is the thickness of the layer. Eq. A.2 shows a matching matrix equation, which matches the forward and reverse traveling electric field amplitudes at boundary (b). r and t are respectively the reflection and transmission Fresnel coefficients for a wave incident from medium (1) to medium (2). The parameters β, r, and t must be modified slightly to model non-normal incidence.[8] Our model calculated transmittance at $\theta=0°$ and reflectance at $\theta=7°$ based on the light traveling through air ($\tilde{n}=1$), an LBL PDAC/TDBC J-aggregate film, the glass slide ($\tilde{n}=1.5$), and then air ($\tilde{n}=1$). From the AFM data, the thickness of deposited physical layers was observed to vary from about 1.4 nm to 2.0 nm per adsorbed layer. Because the glass substrate thickness, d_s, is very large in the wavelength range of interest ($d_s/\lambda >> 1$), we modeled the glass as 1 mm thick and averaged the calculated transmittance and reflectance for 10 glass thickness variations comprising a phase change of 0 to 2π at the wavelength of interest in order to remove interference effects in the substrate. For near-normal incidence calculations, the light from the spectrometer was assumed to be circularly polarized.

The Kramers-Kronig (KK) regressions for finding (n,K) were based on the method outlined by Nitsche and Fritz.[36] The propagation and matching matrix model described above was used to calculate the reflectances and transmittances used in the KK regression. However, to minimize convergence errors introduced by interference in the substrate, we used 100 glass variations comprising a phase change of 0 to 2π at the

wavelength of interest. We used the following approximation of the KK transformation given by Nitsche and Fritz relating n and k:

$$n(\omega_j) \cong n_{offset} + \frac{2}{\pi} P \int_{\omega_L}^{\omega_U} \frac{\omega K(\omega)}{\omega^2 - \omega_j^2} d\omega, \ \omega_L \le \omega_j \le \omega_U \quad \text{(Eq. A.3)}$$

The background contributions of frequencies outside of the measured spectrum are approximated through the use of the n_{offset} term in Eq. A.3. For our regressions, we used n_{offset}=1.7 since we assume that PDAC and TDBC resemble many other organic materials outside of the visible spectrum. Like Nitsche and Fritz, we implemented a Levenberg-Marquardt algorithm for use in optimizing K.[46] Our maximum step size at each iteration was 0.01, which ultimately dictated the resolution of the resulting k spectra. The Cauchy principal value in Eq. A.3 was approximated using Maclaurin's Formula.[47]

Appendix B. Experimental Details for Section III

Stamps were produced using Sylgard 184-brand PDMS (polydimethylsiloxane), made by Dow Corning. The PDMS base and curing agent were mixed 10:1 and cured for over 5 hours at 60° C. To create patterned PDMS stamps, the PDMS mixture was poured onto a silicon master and then cured. In the case of flat stamps, the exposed surface of the PDMS was used due to the rough surface of the Petri dish in which the PDMS was cured. The stamps were cut from the PDMS and mounted on glass slides using commercial fast-cure epoxy.

J-aggregate thin films were produced using layer-by-layer assembly. The J-aggregating cyanine dye used was TDBC. Several polyelectrolytes were used in this study due to the two methods of growing J-aggregate films on PDMS. Method 1 involved PDAC, 35% by weight in water, M_w<100,000 and PSS, poly(sodium-4-styrenesulfonate), M_w~1,000,000 (CAS 25704-18-1). Method 2 involved PAH, poly(allylamine hydrochloride), M_w~70,000 (CAS 71550-12-4). All of the polyelectrolytes were obtained from Sigma-Aldrich.

The dye solvent and rinses for the dye adsorption step were DI water, which had a pH of 5 to 5.5. The effect of pH on TDBC has been documented.[44] Except for the PAH solvent, the polyelectrolyte solvents and rinses for the polyelectrolyte adsorption step were DI water. The PAH solvent was DI water plus 0.01 M sodium chloride, and the pH of the solvent was raised to between 7 and 8 using sodium hydroxide. Sodium chloride was AR-brand from Mallinckrodt. Sodium hydroxide was obtained from EM Science.

A standardized routine was used to prepare the dye and polyelectrolyte solutions. The dye solution was approximately $5x10^{-5}$ M. Once the dye was added to the dye

solvent, the dye bucket was placed in an ultrasonic cleaner to sonicate for 30 minutes. The dye was then mixed with a one-inch magnetic spin bar for 10 minutes, sonicated for 20 minutes, mixed for 5 minutes, and finally sonicated for 5 minutes. The polyelectrolyte solutions were all approximately $3x10^{-2}$ M, measuring by monomeric units. The polyelectrolyte solutions were prepared using the same time intervals for mixing/sonication as the dye solution preparation, except sonication and mixing at each step were swapped. Care was taken throughout the deposition to shield the dye solution and samples from light.

Prior to deposition of PDAC/TDBC films onto the stamps, the mounted PDMS stamps were pretreated. The mounted stamps were treated with oxygen plasma for 2 minutes in a Plasma Preen system. Then, the stamps were soaked in a 1 M sodium hydroxide in DI water solution for 40 minutes. The strong basic solution was used to make the silanol groups on the PDMS surface have a largely negative charge, as described in previous work in LBL films for microfluidic applications.[34,35] The stamps and rack were then dipped in a DI water rinse and finally underwent 2 sequential immersions in cationic and anionic solutions (SICAS) of PDAC and PSS, using the standard adsorption step times. For both methods in this study, the layer-by-layer depositions were performed using an automated Leica Autostainer XL. The cation adsorption step consisted of dipping the slides in cationic solution for 5 minutes and in the three rinses for two minutes, two minutes, and one minute, respectively. The anion adsorption step used the same time intervals as those used in the cation adsorption step. After the pretreatment, the stamps underwent varying numbers of SICAS of PDAC and TDBC to build the J-aggregate thin films.

The stamps used for PAH/TDBC film growth did not undergo any significant pretreatment. The mounted stamps were rinsed with DI water three times prior to deposition to remove dust particles and then left immersed in DI water until the start of the deposition. The first PAH adsorption step was extended to 30 minutes to allow extra time for the initial adsorption of PAH onto PDMS via hydrophobic interactions.[32] The stamps then underwent varying numbers of SICAS of PAH and TDBC to build the J-aggregate thin films.

Upon removal from the stainer, the stamps were blown dry using nitrogen gas. Prior to the stamping, glass substrates were cleaned with a detergent solution (Micro-90), acetone, and isopropanol. The acetone, isopropanol, and methanol used in this study were OmniSolv-brand solvents made by EMD Chemicals. The substrates were then treated with oxygen plasma for six minutes in a Plasma Preen system. The stamps were gently separated from their using tweezers. The stamping procedure was as follows: the stamps were picked up by hand, flipped over, and pressed into contact with the glass substrates. Gentle pressure was applied to the backs of the stamps to remove any air bubbles that might have been trapped between the stamp and substrate. The stamps were left in contact with the glass for at least one minute and then removed by lifting one edge of the stamp and peeling the stamp away from the glass. The transferred films on the glass substrates were then characterized.

Measurements for this study were performed in the MIT Center for Materials Science and Engineering Shared Analytical Lab. The AFM data were collected on a Digital Instruments D3000 Scanning Probe Microscope in tapping mode using phosphorus-doped silicon tips from Veeco. The optical data were collected using a Cary

5E UV-Vis-NIR spectrophotometer. The transmission data were collected with the light beam at normal incidence, $\theta=0°$. The reflectance data were collected in a V-W setup with the light beam incidence at $\theta=7°$ using the Cary Specular Reflectance Accessory in Absolute Reflectivity mode.

The indices of refraction for the films were found using KK relations and numerical regression, modeling the J-aggregate thin film with a thin film dielectric model using propagation and matching matrices. The KK regressions performed and the numerical models used were described in detail in the Appendix A. All films were modeled as a single thin film on a glass substrate, despite any pretreatment components that may have been transferred from PDMS. Due to the likely considerable interpenetration of sequential layers deposited via LBL, a discernable boundary between the PDAC/PSS and PDAC/TDBC in films formed by Method 1 likely did not exist. Therefore, a single complex index of refraction was used to describe the films.

Appendix C. MATLAB Code for Performing Kramers-Kronig Regression

kk.m should be modified to point to the correct reflectance and transmittance data files. Additionally, modifications should be made to kk.m to choose fitting based on either reflectance or transmittance data. Lastly, kk.m should be modified to specify the desired data file names.

Once the above modifications have been made, kk.m is run, producing the data files with fitting results. If the regressions do not converge, the parameters of the search algorithm in levmarq.m or levmarq_trans.m should be changed until convergence is achieved.

With the produced data files with fitting results, the final step is to modify and run kkcalc.m to produced the CSV files with calculated and measured transmittance and reflectance along with the fitted (n,K). The procedure for kkcalc.m is as follows: modify kkcalc.m to specify the desired CSV file name, load a MAT data file produced by kk.m, and run kkcalc.m. Repeat the procedure for each MAT data file produced by kk.m.

kk.m

```
% M. Scott Bradley
% Code for Kramers-Kronig Regression based on
% Reflectance or Transmittance Data

% Adapted from R. Nitsche, T. Fritz, Phys. Rev. B 2004, 70, 195432.

% Constants:
mu0=4*pi*10^-7; % H/m
eps0=8.854*10^-12; % F/m

% CSV files with transmittance and reflectance data, on a scale from 0
to 1
% Format of Files (Column/Data):
% [(1/Wavelength in nm), (2/Energy of Wavelength), (3/Sample1), ...]
CompiledTrans=csvread('C:\MATLAB6p5p1\work\CompiledTrans.csv');
CompiledRefl=csvread('C:\MATLAB6p5p1\work\CompiledRefl.csv');

wavelength=CompiledTrans(:,1)*10^-9; % m
freq=(3*10^8)./wavelength; % Hz
w=2*pi*(3*10^8)./wavelength; % rad/s

energy=(6.626*10^-34)/(1.6*10^-19)*freq; % eV
```

```
% The thickness of the samples is the product of an entry from "layers"
and
% an entry from "dlayers" below.  For cases in which there is a fixed
% thickness/layer, the layer numbers can be specified separate from the
% thickness/layer, which is specified in "dlayers."  This separation
also
% allows several thickness/layer entries to be evaluated in one
execution
% of the script.  If the sample thicknesses are to be separately
specified,
% "layers" should have the thicknesses of the samples in nm, and
"dlayers"
% should have only 1.0.
layers=[1 2 3 4 5 6 7 8 9 10];

Rdata=CompiledRefl(:,3:end);
Rdata=Rdata/100;
Tdata=CompiledTrans(:,3:end);
Tdata=Tdata/100;

Adata=1-Tdata-Rdata; % absorption

noffset=1.7;

%% If needed, the wavelength and energy ranges can be narrowed.
% wavelength=wavelength(1:351);
% energy=energy(1:351);

%%%%%% Cauchy Principal "Integral" Setup %%%%%%
% This is based on the Mclaurin Formula for evaluating the Cauchy
Principal
% value.

% Construct E/(E^2-Ei^2) matrix, called Eterms
% (with zeros on diagonal for E=Ei):
j=1;
for i=1:2:length(energy)-1
    Eodd(j,1)=energy(i);
    j=j+1;
end
j=1;
for i=2:2:length(energy)
    Eeven(j,1)=energy(i);
    j=j+1;
end

dEodd=circshift(Eodd, [-1 0])-Eodd;
dEeven=circshift(Eeven, [-1 0])-Eeven;

Eodd(end)=0;
Eeven(end)=0;
dEodd(end)=0;
dEeven(end)=0;

clear dEs Eranges
dEs(:,1)=dEeven;
Eranges(:,1)=Eeven;
for i=2:length(energy)-3
    if mod(i,2)==0
        Eranges=cat(2,Eranges,Eodd);
        dEs=cat(2,dEs,dEodd);
    else
        Eranges=cat(2,Eranges,Eeven);
        dEs=cat(2,dEs,dEeven);
```

```
    end
end

truncenergy=energy(1:length(energy)-3);

Eterms=Eranges./(Eranges.^2-(ones(size(Eranges))*diag(truncenergy)).^2);

%%%%%%

% "dlayers" matrix.  See comment above "layers" matrix for details.
dlayers=[1.0]; % nm

% evaluate all given thickness/layer entries
for dlayeridx=1:length(dlayers)

    dlayer=dlayers(dlayeridx)*10^-9;

    % Layer=:
    for layeridx=1:length(layers)

        % to be able to resume after breaking
        if useks == 1
            k=kstart(layeridx,:);
        else
            k=zeros(1,length(energy)-1);
        end

        %%%%%% Algorithm for finding KK n,k %%%%%%
        numiterends=zeros(1,length(truncenergy));
        deltak=ones(1,length(truncenergy))*10^-3;
        SQERROR=ones(1,length(truncenergy));
        ktol=0.01;
        iterate=1000;
        idx=0;
        % Require better fitting around J-aggregate peak:
        % for 595, 200:210; for 690 nm dye, 105:115; for 590, 205:215
        while idx < iterate & ...
                (SQERROR(205:215) < (0.001)^2)*ones(11,1) < 11
            idx=idx+1;
%            FOR DEBUGGING:
%            if mod(idx,50) == 0
%                plot(wavelength(1:length(k)),k);
%                pause
%            end

            % Find n(E):
            % Shift k matrix around appropriately:
            kreshaped=reshape(k,[2,length(k)/2]);
            kshiftdim=shiftdim(kreshaped,1);
            kcirc=circshift(kshiftdim,[0 1]);
            ktiled=repmat(kcirc,1,length(truncenergy)/2);

            % Perform sum to finish Maclaurin's formula:
            sumterms=2/pi*ktiled.*Eterms.*dEs;
            n=noffset+2/pi*sum(sumterms);

            for i=1:length(n)
%                 DEBUG INFORMATION:
                idx
                wavelength(i)

                %%% Transmittance or Reflectance?
                %%% The implementation shown below is for transmittance.
```

```
                %%% To run this script on reflectance data, levmarq
should
                %%% be used instead of levmarq_trans, and Tdata and T
                %%% should be swapped with Rdata and R, respectively, in
                %%% the calculation of the new SQERROR entry.
                %%%
                %%% The script assumes that the measurements are normal
                %%% (0-degree) transmittance and near-normal (7-degree)
                %%% reflectance.
                [knew,iterend,SQERROR(i),deltak(i)]= ...
                    levmarq_trans(wavelength(i), ...
                    layers(layeridx)*dlayer, n(i), k(i), ...
                    Tdata(i,layeridx),deltak(i));
                if abs(knew-k(i)) > ktol
                    if (knew-k(i)) < 0
                        k(i)=k(i)-ktol;
                        [T, t7, r, R]=slow_coefficients( ...
                            layers(layeridx)*dlayer, wavelength(i), ...
                            n(i), k(i));
                        SQERROR(i)=abs(Tdata(i,layeridx)-T)^2;
                    else
                        k(i)=k(i)+ktol;
                        [T, t7, r, R]=slow_coefficients( ...
                            layers(layeridx)*dlayer, wavelength(i), ...
                            n(i), k(i));
                        SQERROR(i)=abs(Tdata(i,layeridx)-T)^2;
                    end
                end
                if iterend > 0
                    numiterends(i)=numiterends(i)+iterend;
                end
            end
        end

        %%%%%% Output data to a .mat file.
        basefilename='kkspectrum_date_experimentdescription';
        filename=sprintf('%s_%1.1fnmperlayer_%1.1flayers.mat',...
            basefilename,dlayers(dlayeridx),layers(layeridx));
        save(filename);
    end
end
```

levmarq.m

```
% M. Scott Bradley
% Implementation of Levenberg-Marquardt algorithm for use in varying n
% based on k (using reflectance data):

function [k,iterend,SQERROR,deltaknew]=levmarq(lambda,d,n,kstart,...
    Rexp,deltak0)

k0=kstart;

deltak=deltak0;

% LM algorithm parameters:
v=10;

lamda=0.1;
i=0;

[t, t7, r, R0]=slow_coefficients(d, lambda, n, k0);

[t, t7, r, Rplus]=slow_coefficients(d, lambda, n, k0+deltak);
```

```
[t, t7, r, Rminus]=slow_coefficients(d, lambda, n, k0-deltak);
deriv1=(Rplus-Rminus)/(2*deltak);

SQERROR=(Rexp-R0)^2;

if deriv1==0
    k=k0;
    iterend=10000;
    deltaknew=deltak0;
    return;
end

% Don't be fooled by a past mistake here.  Secderiv is just the Jacobian
% squared, which approximates the second derivative.
secderiv=deriv1^2;

delta=(deriv1*(Rexp-R0))/(secderiv+lamda*deriv1);
deltav=(deriv1*(Rexp-R0))/(secderiv+lamda*deriv1/v);

k0=k0+delta;
k0v=k0+deltav;
[t, t7, r, R0]=slow_coefficients(d, lambda, n, k0);
[t, t7, r, R0v]=slow_coefficients(d, lambda, n, k0v);
PHI0v=(Rexp-R0v)^2;
PHI0=(Rexp-R0)^2;

iterate=100;

while PHI0 > (0.01)^2 & i < iterate
    i=i+1;

    [t, t7, r, Rplus]=slow_coefficients(d, lambda, n, k0+deltak);
    [t, t7, r, Rminus]=slow_coefficients(d, lambda, n, k0-deltak);
    deriv1=(Rplus-Rminus)/(2*deltak);

    if deriv1==0
        k=k0;
        iterend=10000;
        deltaknew=deltak0;
        return;
    end

    secderiv=deriv1^2;
    delta=(deriv1*(Rexp-R0))/(secderiv+lamda*secderiv);

    k1=k0+delta;

    [t, t7, r, R1]=slow_coefficients(d, lambda, n, k1);

    PHI1=(Rexp-R1)^2;

    if PHI0v <= PHI1
        lamda = lamda/v;
    elseif PHI0v > PHI1 & PHI0 < PHI1
        lamda = lamda;
    else
        while PHI1 > PHI0
            lamda = lamda*v;
            delta=(deriv1*(Rexp-R0))/(deriv1^2+lamda*deriv1^2);
            k1=k0+delta;
            [t, t7, r, R1]=slow_coefficients(d, lambda, n, k1);
            PHI1=(Rexp-R1)^2;
        end
    end
```

```
    delta=(deriv1*(Rexp-R0))/(secderiv+lamda*secderiv);
    deltav=(deriv1*(Rexp-R0))/(secderiv+lamda*secderiv/v);
    k1=k0+delta;
    k1v=k0+deltav;
    [t, t7, r, R1]=slow_coefficients(d, lambda, n, k1);
    [t, t7, r, R1v]=slow_coefficients(d, lambda, n, k1v);
    PHI1=(Rexp-R1)^2;
    PHI1v=(Rexp-R1v)^2;

    if abs(delta/2) < deltak
        deltak=abs(delta/2);
    end

    k0=k1;
    R0=R1;
    PHI0=PHI1;
    PHI0v=PHI1v;
end

k=k0;
SQERROR=PHI0;
iterend=(i==iterate);
deltaknew=deltak;
```

levmarq_trans.m

```
% M. Scott Bradley
% Implementation of Levenberg-Marquardt algorithm for use in varying n
% based on k (using transmittance data):

function
[k,iterend,SQERROR,deltaknew]=levmarq_trans(lambda,d,n,kstart,...
    Texp,deltak0)

k0=kstart;

deltak=deltak0;

% LM algorithm parameters:
v=10;
lamda=0.01;

i=0;

[T0, t7, r, r7]=slow_coefficients(d, lambda, n, k0);

[Tplus, t7, r, r7]=slow_coefficients(d, lambda, n, k0+deltak);
[Tminus, t7, r, r7]=slow_coefficients(d, lambda, n, k0-deltak);
deriv1=(Tplus-Tminus)/(2*deltak);

SQERROR=(Texp-T0)^2;

if deriv1==0
    k=k0;
    iterend=10000;
    deltaknew=deltak0;
    return;
end

% Don't be fooled by a past mistake here.  Secderiv is just the Jacobian
% squared, which approximates the second derivative.
secderiv=deriv1^2;
```

```
delta=(deriv1*(Texp-T0))/(secderiv+lamda*deriv1);
deltav=(deriv1*(Texp-T0))/(secderiv+lamda*deriv1/v);

k0=k0+delta;
k0v=k0+deltav;
[T0, t7, r, r7]=slow_coefficients(d, lambda, n, k0);
[T0v, t7, r, r7]=slow_coefficients(d, lambda, n, k0v);
PHI0v=(Texp-T0v)^2;
PHI0=(Texp-T0)^2;

iterate=100;

while PHI0 > (0.01)^2 & i < iterate
    i=i+1;

    [Tplus, t7, r, r7]=slow_coefficients(d, lambda, n, k0+deltak);
    [Tminus, t7, r, r7]=slow_coefficients(d, lambda, n, k0-deltak);
    deriv1=(Tplus-Tminus)/(2*deltak);

    if deriv1==0
        k=k0;
        iterend=10000;
        deltaknew=deltak0;
        return;
    end

    secderiv=deriv1^2;
    delta=(deriv1*(Texp-T0))/(secderiv+lamda*secderiv);

    k1=k0+delta;

    [T1, t7, r, r7]=slow_coefficients(d, lambda, n, k1);

    PHI1=(Texp-T1)^2;

    if PHI0v <= PHI1
        lamda = lamda/v;
    elseif PHI0v > PHI1 & PHI0 < PHI1
        lamda = lamda;
    else
        while PHI1 > PHI0
            lamda = lamda*v;
            delta=(deriv1*(Texp-T0))/(deriv1^2+lamda*deriv1^2);
            k1=k0+delta;
            [T1, t7, r, r7]=slow_coefficients(d, lambda, n, k1);
            PHI1=(Texp-T1)^2;
        end
    end

    delta=(deriv1*(Texp-T0))/(secderiv+lamda*secderiv);
    deltav=(deriv1*(Texp-T0))/(secderiv+lamda*secderiv/v);
    k1=k0+delta;
    k1v=k0+deltav;
    [T1, t7, r, r7]=slow_coefficients(d, lambda, n, k1);
    [T1v, t7, r, r7]=slow_coefficients(d, lambda, n, k1v);
    PHI1=(Texp-T1)^2;
    PHI1v=(Texp-T1v)^2;

    if abs(delta/2) < deltak
        deltak=abs(delta/2);
    end

    k0=k1;
```

```
    T0=T1;
    PHI0=PHI1;
    PHI0v=PHI1v;
end

k=k0;
SQERROR=PHI0;
iterend=(i==iterate);
deltaknew=deltak;
```

slow_coefficients.m

```
% M. Scott Bradley
% Function for using propagation and matching matrices to find normal
and
% 7-degree transmission and reflection coefficients.

% This is "slow_coefficients" because the glass variations are averaged
% using a for loop.  If a range of n and k are to be used, then the
% averaging can be sped up by using a large matrix and doing all of the
% variations in one pass (without for loops, which are slow for MATLAB).

% d is thickness, lambda is wavelength, n and k are J-Agg optical
constants
function [t,t7,r,r7] = coefficients(d, lambda, n, k)

% Constants:
mu0=4*pi*10^-7; % H/m
eps0=8.854*10^-12; % F/m

% Measurement Parameters:
omega=2*pi*(3*10^8)/lambda; % rad/s
k0=2*pi/lambda; % wave vector in air
kx=k0*sin(7*pi/180); % x-component of the wave vector in air
theta1=7*pi/180; % initial angle (can be changed when angle is variable)

% J-Aggregate Parameters:
% This minus is reflected in the sign of beta in the propagation
% matrices...(effect from the Ward book).
nJAgg=n-j*k;

kGlass=sqrt(omega^2*mu0*1.5^2*eps0); % wave vector, without angle, in
glass
glassvar=[0:2*pi/100:2*pi]/kGlass; % glass variations to average

% Based on "The Optical Constants of Thin Films and Bulk Materials" by
Ward

% At 7 degree incidence:
% First, TE case:

% (1) Air to J-Aggregate Matching Matrix:
% Find u2-j*v2 for ~n2*cos(theta2):
u2=sqrt(0.5*((n^2-k^2)-sin(theta1)^2+(((n^2-k^2)-...
    sin(theta1)^2)^2+(2*n*k)^2)^0.5));
v2=sqrt(0.5*(sin(theta1)^2-(n^2-k^2)+(((n^2-k^2)-...
    sin(theta1)^2)^2+(2*n*k)^2)^0.5));

rho1=(1*cos(theta1)-(u2-j*v2))/(1*cos(theta1)+(u2-j*v2));
tau1=(2*1*cos(theta1))/(1*cos(theta1)+u2-j*v2);

T1=(1/tau1)*[1 rho1; rho1 1];
```

```
% (2) J-Aggregate Propagation Matrix:
%kJAgg=sqrt(omega^2*mu0*epsJAgg); epsJAgg=(n-j*k)^2*eps0

T2=[exp(j*sqrt(omega^2*mu0*eps0)*(u2-j*v2)*d) 0; ...
    0 exp(-j*sqrt(omega^2*mu0*eps0)*(u2-j*v2)*d)];

% (3) J-Aggregate to Glass Matching Matrix:
theta3=asin(sqrt(n^2-k^2-u2^2+v2^2)/1.5);

rho3=((u2-j*v2)-1.5*cos(theta3))/((u2-j*v2)+1.5*cos(theta3));
tau3=(2*(u2-j*v2))/(1.5*cos(theta3)+(u2-j*v2));

T3=(1/tau3)*[1 rho3; rho3 1];

% Will iterate through glass propagation matrices later
% (4) Glass to Air Matching Matrix
theta4=asin((1.5/1)*sin(theta3));

rho4=(1.5*cos(theta3)-1*cos(theta4))/(1*cos(theta4)+1.5*cos(theta3));
tau4=(2*1.5*cos(theta3))/(1*cos(theta4)+1.5*cos(theta3));

T4=(1/tau4)*[1 rho4; rho4 1];

% Putting it all together, sum over all the glass thicknesses to cancel
out
% the glass phase variations.
sumrTE7=0;
sumtTE7=0;
for q=1:length(glassvar)
    beta=cos(theta3)*(10^-3+glassvar(q));
    T3a=[exp(j*kGlass*beta) 0; 0 exp(-j*kGlass*beta)];
    Ttot=T1*T2*T3*T3a*T4;

    E1ref=Ttot*[1;0];
    RTE7temp=(abs(E1ref(2))/abs(E1ref(1)));
    % For transmission coefficient, we have to solve for E2'+/E1+, which
is
    % just 1/Ttot(1,1):
    TTE7temp=abs(1/Ttot(1,1));

    sumrTE7=sumrTE7+RTE7temp^2;
    sumtTE7=sumtTE7+TTE7temp^2;
end

rTE7=sumrTE7/length(glassvar);
tTE7=sumtTE7/length(glassvar);

% Next, TM case:

% (1) Air to J-Aggregate Matching Matrix:
theta1=7*pi/180;

rho1=((n^2-k^2)*cos(theta1)-u2-j*(2*n*k*cos(theta1)-v2))/...
    ((n^2-k^2)*cos(theta1)+u2-j*(2*n*k*cos(theta1)+v2));
tau1=(2*(n-j*k))/((u2-j*v2)/cos(theta1)+(n-j*k)^2);

T1=(1/tau1)*[1 rho1; rho1 1];

% (2) J-Aggregate Propagation Matrix:
%kJAgg=sqrt(omega^2*mu0*epsJAgg);

T2=[exp(j*sqrt(omega^2*mu0*eps0)*(u2-j*v2)*d) 0;...
    0 exp(-j*sqrt(omega^2*mu0*eps0)*(u2-j*v2)*d)];
```

```
% (3) J-Aggregate to Glass Matching Matrix:
theta3=asin(sqrt(n^2-k^2-u2^2+v2^2)/1.5);

rho3=(1.5*u2-(n^2-k^2)*cos(theta3)-j*(1.5*v2-2*n*k*cos(theta3)))/...
    (1.5*u2+(n^2-k^2)*cos(theta3)-j*(1.5*v2+2*n*k*cos(theta3)));
tau3=(2*(n-j*k)*(u2-j*v2))/((n-j*k)^2*cos(theta3)+1.5*(u2-j*v2));

T3=(1/tau3)*[1 rho3; rho3 1];

% Will iterate through glass propagation matrices later

% (4) Glass to Air Matching Matrix
theta4=asin((1.5/1)*sin(theta3));

rho4=(1.5/cos(theta3)-1/cos(theta4))/(1/cos(theta4)+1.5/cos(theta3));
tau4=(2*1.5/cos(theta3))/(1/cos(theta4)+1.5/cos(theta3));

T4=(1/tau4)*[1 rho4; rho4 1];

% Putting it all together, sum over all the glass thicknesses to cancel
out
% the glass phase variations.
sumrTM7=0;
sumtTM7=0;
for q=1:length(glassvar)
    beta=cos(theta3)*(10^-3+glassvar(q));
    T3a=[exp(j*kGlass*beta) 0; 0 exp(-j*kGlass*beta)];
    Ttot=T1*T2*T3*T3a*T4;

    E1ref=Ttot*[1;0];
    RTM7temp=(abs(E1ref(2))/abs(E1ref(1)));
    TTM7temp=abs(1/Ttot(1,1));

    sumrTM7=sumrTM7+RTM7temp^2;
    sumtTM7=sumtTM7+TTM7temp^2;
end

rTM7=sumrTM7/length(glassvar);
tTM7=sumtTM7/length(glassvar);

r7=(rTM7+rTE7)/2;
t7=(tTM7+tTE7)/2;

% At normal incidence

% (1) Air to J-Aggregate Matching Matrix:
rho1=(1-nJAgg)/(1+nJAgg);
tau1=(2*1)/(1+nJAgg);

T1=(1/tau1)*[1 rho1; rho1 1];

% (2) J-Aggregate Propagation Matrix:
kJAgg=omega*nJAgg*sqrt(mu0*eps0);

T2=[exp(j*kJAgg*d) 0; 0 exp(-j*kJAgg*d)];

% (3) J-Aggregate to Glass Matching Matrix:
rho3=(nJAgg-1.5)/(nJAgg+1.5);
tau3=(2*nJAgg)/(1.5+nJAgg);

T3=(1/tau3)*[1 rho3; rho3 1];

% Will iterate through glass propagation matrices later
```

```
% (4) Glass to Air Matching Matrix
rho4=(1.5-1)/(1+1.5);
tau4=(2*1.5)/(1+1.5);

T4=(1/tau4)*[1 rho4; rho4 1];

% Putting it all together, sum over all the glass thicknesses to cancel
out
% the glass phase variations.
sumr=0;
sumt=0;
for q=1:length(glassvar)
    beta=10^-3+glassvar(q);
    T3a=[exp(j*kGlass*beta) 0; 0 exp(-j*kGlass*beta)];
    Ttot=T1*T2*T3*T3a*T4;

    E1ref=Ttot*[1;0];
    Rtemp=(abs(E1ref(2))/abs(E1ref(1)));
    Ttemp=abs(1/Ttot(1,1));

    sumr=sumr+Rtemp^2;
    sumt=sumt+Ttemp^2;
end

r=sumr/length(glassvar);
t=sumt/length(glassvar);
```

kkcalc.m

```
% M. Scott Bradley
% Script to calculate R,T spectrum from KK spectrum data; depends on
data
% from a kk.m run

if length(k) < length(n)
    wavelim=length(k);
else
    wavelim=length(n);
end

for idx1=1:wavelim
    wavelength(idx1)

    [tcalc(idx1), t7calc(idx1), rcalc(idx1), r7calc(idx1)]=...
        slow_coefficients(dlayer*layers(layeridx), wavelength(idx1), ...
            n(idx1),k(idx1));
end

% For exporting to Origin:
M=wavelength(1:length(n));

%% For input data with just R:
% M=cat(2,M,Rdata(1:length(n),layeridx), r7calc', ...
%     tcalc', n', k(1:length(n))');

%% only transmission, ignoring r7calc
% M=cat(2,M, Tdata(1:length(n),layeridx), tcalc', n', k(1:length(n))');

% For input data with both R and T:
M=cat(2,M,Rdata(1:length(n),layeridx), r7calc', ...
    Tdata(1:length(n),layeridx), tcalc', n', k(1:length(n))');

csvwrite('kkspectrum_20051206_pahtdbcstamps_trans_1SICAS.csv',M);
```

Bibliography

[1] D. G. Lidzey, D. D. C. Bradley, M. S. Skolnick, T. Virgili, S. Walker, D. M. Whittaker, *Nature* **1998**, *395*, 53.

[2] D. G. Lidzey, D. D. C. Bradley, T. Virgili, A. Armitage, M. S. Skolnick, S. Walker, *Phys. Rev. Lett.* **1999**, *82*, 3316.

[3] C. Weisbuch, M. Nishioka, A. Ishikawa, Y. Arakawa, *Phys. Rev. Lett.* **1992**, *69*, 3314.

[4] P. Schouwink, H. V. Berlepsch, L. Dahne, R. F. Mahrt, *Chem. Phys. Lett.* **2001**, *344*, 352.

[5] C. Weisbuch, H. Benisty, R. Houdre, *J. Lumin.* **2000**, *85*, 271.

[6] J. R. Tischler, "Electrically pumped polariton emission in a J-aggregate organic light emitting device," Massachusetts Institute of Technology, Cambridge, MA **2003**.

[7] J. R. Tischler, M. S. Bradley, V. Bulovic, J. H. Song, A. Nurmikko, *Phys. Rev. Lett.* **2005**, *95*, 036401.

[8] R. S. Eachus, A. P. Marchetti, A. A. Muenter, *Annu. Rev. Phys. Chem.* **1999**, *50*, 117.

[9] E. E. Jelley, *Nature* **1936**, *138*, 1009.

[10] G. Scheibe, *Z. Angew. Chem.* **1936**, *49*, 563.

[11] H. Kuhn, C. Kuhn, in *J-Aggregates*, (Eds: T. Kobayashi), World Scientific Publishing Co. Pte. Ltd., Singapore **1996**, pp 1-40.

[12] D. F. O'Brien, *Photo. Sci. Eng.* **1974**, *18*, 16.

[13] K. Misawa, H. Ono, K. Minoshima, T. Kobayashi, *Appl. Phys. Lett.* **1993**, *63*, 577.

[14] H. Fukumoto, Y. Yonezawa, *Thin Solid Films* **1998**, *327-329*, 748.

[15] G. Decher, J. D. Hong, *Makromol. Chem., Macromol. Symp.* **1991**, *46*, 321.

[16] G. Decher, J. D. Hong, *Berichte der Bunsen-Gesellschaft* **1991**, *95*, 1430.

[17] G. Decher, J. D. Hong, J. Schmitt, *Thin Solid Films* **1992**, *210-211*, 831.

[18] G. Decher, *Science* **1997**, *277*, 1232.

[19] G. Decher, in *Multilayer Thin Films*, (Eds: G. Decher, J. B. Schlenoff), Wiley-VCH Verlag GmbH & Co. KGaA, Weinheim **2002**, pp 1-46.

[20] K. Ariga, Y. Lvov, T. Kunitake, *J. Am. Chem. Soc.* **1997**, *119*, 2224.

[21] A. Naber, U. C. Fischer, S. Kirchner, T. Dziomba, G. Kollar, L. F. Chi, H. Fuchs, *J. Phys. Chem. B* **1999**, *103*, 2709.

[22] C. Peyratout, L. Daehne, *Phys. Chem. Chem. Phys.* **2002**, *4*, 3032.

[23] M. Kawasaki, T. Sato, T. Yoshimoto, *Langmuir* **2000**, *16*, 5409.

[24] M. Orrit, D. Möbius, U. Lehmann, H. Meyer, *J. Chem. Phys.* **1986**, *85*, 4966.

[25] H. Kuhn, D. Möbius, H. Bücher, in *Physical Methods of Chemistry: Part IIIB Optical, Spectroscopic, and Radioactivity Methods*, (Eds: A. Weissberger, B. Rossiter), Wiley-Interscience, New York **1972**.

[26] L. Dahne, A. Horvath, G. Weiser, *Chem. Phys.* **1993**, *178*, 449.

[27] M. Vacha, M. Saeki, M. Furuki, L. S. Pu, K.-i. Hashizume, T. Tani, *J. Lumin.* **2002**, *98*, 35.

[28] R. Stepniewski, K. P. Korona, A. Wysmolek, J. M. Baranowski, K. Pakula, M. Potemski, G. Martinez, I. Grzegory, S. Porowski, *Phys. Rev. B* **1997**, *56*, 15151.

[29] R. N. Philp, D. R. Tilley, *Phys. Rev. B* **1991**, *44*, 8170.

[30] J. J. Hopfield, *Phys. Rev.* **1958**, *112*, 1555.
[31] P. T. Hammond, *Adv. Mater.* **2004**, *16*, 1271.
[32] J. Park, P. T. Hammond, *Adv. Mater.* **2004**, *16*, 520.
[33] M. S. Bradley, J. R. Tischler, V. Bulovic, *Adv. Mater.* **2005**, *17*, 1881.
[34] H. Makamba, J. H. Kim, K. Lim, N. Park, J. H. Hahn, *Electrophoresis* **2003**, *24*, 3607.
[35] H. Katayama, Y. Ishihama, N. Asakawa, *Anal. Chem.* **1998**, *70*, 2254.
[36] R. Nitsche, T. Fritz, *Phys. Rev. B* **2004**, *70*, 195432.
[37] A. Kumar, G. M. Whitesides, *Appl. Phys. Lett.* **1993**, *63*, 2002.
[38] J. L. Wilbur, A. Kumar, E. Kim, G. M. Whitesides, *Adv. Mater.* **1994**, *6*, 600.
[39] A. Kumar, H. A. Biebuyck, G. M. Whitesides, *Langmuir* **1994**, *10*, 1498.
[40] B. D. Gates, Q. B. Xu, M. Stewart, D. Ryan, C. G. Willson, G. M. Whitesides, *Chem. Rev.* **2005**, *105*, 1171.
[41] M. Geissler, Y. N. Xia, *Adv. Mater.* **2004**, *16*, 1249.
[42] Y. N. Xia, J. A. Rogers, K. E. Paul, G. M. Whitesides, *Chem. Rev.* **1999**, *99*, 1823.
[43] Y. N. Xia, G. M. Whitesides, *Annual Review of Materials Science* **1998**, *28*, 153.
[44] I. A. Struganova, H. Lim, S. A. Morgan, *J. Phys. Chem. B* **2002**, *106*, 11047.
[45] L. Ward, *The Optical Constants of Bulk Materials and Films*, IOP Publishing Ltd., Bristol, UK **1994**.
[46] D. W. Marquardt, *J. Soc. Ind. Appl. Math* **1963**, *11*, 431.
[47] K. Ohta, H. Ishida, *Appl. Spectrosc.* **1988**, *42*, 952.